

## CHAPTER E-1 CONCRETE PROPERTY CONSIDERATIONS

### E-1.1 Key Concepts

In order to assess concrete structures, reasonable concrete material properties must be determined or estimated. Concrete is a mixture of cement, water, fine aggregate, coarse aggregate, and admixtures. The properties of the concrete will be dependent on the properties of the component parts, the relative proportion of each, the placement methods, the curing conditions during construction, and the curing conditions during the life of the project. This results in a complex material with significant variability in the properties between projects and between samples of the same mix design. Because of this, mix design practices have been developed that consider this variability and ensure adequate performance consistent with design strength assumptions. A risk assessment seeks to understand the actual behavior of a structure in its current state, and should therefore attempt to determine the mean concrete properties and to understand the variability of the concrete properties when determining the probability of failure of a structure.

This chapter will provide guidance on establishing commonly needed concrete properties for the evaluation of dams and levees. The properties will therefore be focused on conventional mass concrete construction, though many aspects are applicable to reinforced concrete, roller compacted concrete, and other concrete construction methods as well. Mass concrete structures typically do not fail in compression, however the compressive strength is a helpful property to correlate to other properties that will matter much more in the failure of the structure. In order to understand the response of concrete structures the tensile strength and shear strength are typically very important. Methods for estimating tensile strength are discussed in this chapter, however there are many factors at play and there is no universally accepted method for determining this property. The shear capacity of mass concrete structures is needed for the stability and shear strength evaluation of structures. The shear strength of mass concrete structures placed in lifts, while somewhat dependent on the strength of the concrete, is highly dependent on the construction methods, such as joint cleanup, placement methods, etc.



## **E-1.2 General Considerations**

### **E-1.2.1 Type of Concrete Construction**

The first consideration when beginning a risk assessment is the type of concrete construction that is being evaluated. Many conclusions can be drawn about the likely properties of the structure with this information. The main types of concrete construction that the material properties discussed in this chapter will be applicable to are discussed in the following sections.

#### **E-1.2.1.1 Conventional Reinforced Concrete**

Conventional reinforced concrete is characterized by Portland cement concrete with relatively small coarse aggregate with sizes generally less than 1.5 inches. The size of the aggregate is controlled by the reinforcement spacing and the placement method. Concrete members subjected to bending, axial, and shear forces can be constructed using conventional reinforced concrete, and typically will rely on the reinforcement to carry all member tensile stresses. This means that in cases where a large amount of reinforcement is needed, the maximum coarse aggregate size will be small so that the concrete can be effectively placed around the reinforcement. Placement methods will also affect the size of the aggregate and may require other admixtures. For example, to prevent damage to the lines, pump trucks will require a smaller aggregate size than placement directly from an agitator truck or a bucket. The strength of the concrete will vary based on the purpose of the structure, but for structures typically found at dam and levee projects, the specified strength is typically in the range of 3000 to 5000 psi within 28 days of placement. Some special application of conventional reinforced concrete, such as precast concrete construction, may require a higher strength. Conventional reinforced concrete is a common material used to construct appurtenant features at dams (spillway piers, training walls, stilling basins, etc.) and is a common material used for floodwalls for flood protection projects. Additional information on reinforced concrete can be found in Chapter E-2.

#### **E-1.2.1.2 Prestressed and Post-Tensioned Reinforced Concrete**

Prestressed concrete is a precast concrete construction method where high strength strands are stressed and cast into a concrete member. Once the concrete has gained enough strength, the strands are released to transfer their prestress load into the concrete. This places the concrete in a state of compression which will increase the flexural and/or tension loading the member can

withstand without cracking and reduces deflections. In order to withstand the higher compressive loads that the member will be expected to experience, prestressed concrete typically has a higher strength than conventional reinforced concrete. The higher compressive strength also reduces the creep in the concrete. Creep in the concrete will reduce the amount of prestress over time.

Prestressed concrete is commonly used for spillway bridges on dams and can be used for certain types of floodwalls, but is less common than conventional reinforced concrete.

Post-tensioned concrete is allowed to cure, and then high strength strands or reinforcing bars are installed, stressed against the structure, and permanently locked off to maintain the stress in the structure. Post-tensioning is used to increase the load carrying capacity of a system without increasing the movement of the structure. Post-tensioned concrete is commonly used as trunnion anchorages for radial spillway gates and to increase the stability of existing structures such as gravity dams. Similar to prestressed concrete, a higher strength is often required for new construction. It is therefore common for the zone of concrete in a spillway pier that contains the trunnion anchorage to be constructed of a higher strength concrete mix.

#### **E-1.2.1.3      Conventional Mass Concrete**

Conventional mass concrete is often used for gravity structures that do not need to withstand significant tensile stresses under normal loading. Since the structure does not need to withstand significant tensile stresses, mass concrete structures are typically unreinforced except in areas that are tied to other reinforced concrete structures. Because these are gravity structures, they must be massive in order to resist the applied lateral loads. The mass concrete placements required to construct the structure generate significant heat of hydration and volume changes. To combat these issues lower strengths are typically used in order to reduce the amount of cement. The Portland cement is often supplemented with other cementitious materials such as natural and manmade pozzolans. Most commonly fly ash is used because this improves the workability of the concrete, reduces the heat of hydration, and slows the strength gain. This results in lower specified strengths on the order of 1500-2000 psi at 28 days. Additionally, given the long construction period and low cement content, it is also typical to have required strength gain times longer than the standard 28 days used for reinforced concrete structures. Attaining the specified strength in 90 days or longer is common for conventional mass concrete specifications. A typical

90-day specified strength for a mass concrete structure may be on the order of 2500 to 3500 psi. Reducing the Portland cement content alone will often not be sufficient to control the heat of hydration depending on the size of the project. In these cases other measures such as cooling the aggregate, replacing mix water with ice, mixing liquid nitrogen in the batches, nighttime placement, and embedding cooling coils in the concrete may be used. To control the volume changes associated with the heat of hydration and the curing process, the aggregate size is generally larger than in conventional reinforced concrete (up to six inches). For large structures such as dams, the amount of specialized concrete to be placed often requires an onsite concrete plant and specialized placement procedures. Mass concrete is also placed in lifts of typically 5-10 feet, which creates specialized placement procedures to ensure that a good bond is achieved between the lifts.

#### **E-1.2.1.4      Roller Compacted Concrete**

Roller compacted concrete (RCC) is a dry concrete mix with zero slump. This gives the placed concrete enough stiffness that it can be consolidated by vibratory rollers. The placement methods for roller compacted concrete makes this type of concrete amenable to large placements with shorter construction durations, making the material a relatively inexpensive alternative to conventional mass concrete for large gravity structures. The resulting concrete can sometimes result in lower strengths than conventional mass concrete; however, depending on the mix design, the mechanical properties of roller compacted concrete may be very similar to conventional mass concrete. Because of the dry mix and placement methods, RCC is typically more permeable than conventional mass concrete. For water retention structures such as dams and floodwalls, this can be problematic. RCC is well suited for large structures that do not require a low permeability, such as energy dissipation structures. To reduce the permeability of an RCC structure, it is common for interior concrete to use roller compacted concrete and surficial/facing concrete to use conventional mass concrete. This means that mechanical properties of the structure may be very close to that of conventional mass concrete. Other means of improving the permeability would include applying an impervious coating or sheeting to the upstream face of the structure. In this case, the mechanical properties may be different from mass concrete, depending on the particular mix design. Some guidance is given in this chapter for RCC, but the estimated RCC properties used for a given assessment must be evaluated on a case-

by-case basis after assessing the mix design and construction methods. More information on the material properties for RCC can be found in EP 1110-2-12 (USACE, 1995) and RCC Design and Construction Considerations for Hydraulic Structures (USBR, 2005).

#### **E-1.2.2 Date of Construction**

Risk assessments will generally be performed on existing structures. Many times there will be limited information from the original design regarding the properties of interest for the evaluation of the structure. For this reason, the risk assessment team must use all available information to estimate the properties of the structure. One key piece of information will be the date that the structure was constructed. Based on this information judgments can be made based on the concrete technology and practices common at the time. An abbreviated list of significant advancements is given in Table E-1-1.

**Table E-1-1 Timeline of Advances in Concrete Technology**

<b>Date</b>	<b>Advancement</b>
1905-1910	Reinforced concrete used
1929	Basic principles of concrete material implemented
1933	Internal vibration of concrete used
1930's	Air entrainment of concrete
Late 1940's	ASR reducing practices implemented
1967	Sulfate attack virtually eliminated

In addition to the date of construction, the historical data and files developed throughout the life of the structure should be reviewed for any additional information. The best information on an existing structure will come from recent core reports. If the relevant testing for the needed material properties was completed based on recent cores this will give the current properties of

the concrete, which will be the most helpful in performing an evaluation. Older core reports may also be helpful. Though these older reports may not give the current properties of the concrete, they do give insight into the in situ properties. The field data and construction practices for the original construction should also be reviewed. There may be records of materials used and mixture proportions that can be used to estimate some properties. There may also be records of strength development after placements of concrete which can be informative in determining the current strength of the concrete. Lastly, there may be lab investigations from the original mix design. These lab investigations must be used carefully since they may have tested numerous mix designs and the material used in the final mix may have been changed during construction. Additionally, there is often a difference between lab cured concrete cylinders versus samples cored from an actual structure that would have experienced different curing conditions.

### **E-1.3 Compressive Strength**

The compressive strength of concrete is one of the primary properties of focus for a mix design. Because concrete gains strength gradually as the hydration reaction of the cement takes place, the compressive strength will be different depending on when a sample is tested. Typically structural concrete is required to reach its specified target design compressive strength with 28 days of curing. Thus the design compressive strength ( $f_c'$ ) typically refers to a 28-day strength. As noted previously, the material properties of concrete can vary significantly from sample to sample. This requires conservatism in both the mix design and the acceptance criteria for concrete tested during construction. For example, the acceptance criteria required by ACI 318 is that the arithmetic average of any three consecutive compressive strength tests equals or exceeds  $f_c'$  and no strength test falls below  $f_c'$  by more than 500 psi (or  $0.1f_c'$  if  $f_c'$  exceeds 5000 psi). In order to meet this requirement the mean strength of the concrete must be somewhat higher than the specified strength. ACI 214 gives recommendations for setting the mean based on past statistical evaluation of a mix design, however a common practice is to set the target mean of a mix design to 1.34 standard deviations above the specified strength. In the absence of actual data, a reasonable standard deviation for a given mix design is 15% of the mean strength. It follows from this that, without better data, it can be assumed that the average concrete strength will be approximately 1.25 times the specified strength.

The previous discussion demonstrated that the test cylinders cured in a lab will have an average strength higher than the specified strength. However, the lab curing conditions are different than that in the field. The primary difference is the high surface area to volume ratio of lab cured samples compared to a mass concrete placement. Because of this, the 28 day strength of concrete cored from the structure is generally found to be somewhat greater than the 28 day strength of lab cured samples of the same mix design (USB, 1981). Additionally, the 28 day strength does not represent the maximum strength of the concrete. Generally as long as the relative humidity in the concrete is above 80% with favorable temperatures, the concrete will continue to cure and gain strength for many years, albeit at a continuously decreasing rate (Jansen, 1988). Dam and levee structures would typically be in a humid environment, so it is reasonable to expect continued strength gain in these structures beyond their specified curing time. Numerous authors have attempted to quantify the strength gain of concrete through the life of a structure. The rate of strength gain has been found to be a function of the cement type used in the mix design. Equation E-1-1 can be used to estimate the strength at any desired future time based on the strength at any other previous time (CEB-FIP Model Code, 1990). The cement dependent coefficient,  $s$ , is given in

Table E-1-2 which was fit to data from the Coastal Engineering Manual (EM 1110-2-1100) and Wood (1992). Equation E-1-1 is plotted along with the data from Wood (1992) in order to show the variability in the estimate of strength gain.

$$f_{c,t_2} = f_{c,t_1} e^{s \left( 1 - \sqrt{\frac{t_1}{t_2}} \right)} \quad \text{Equation E-1-1}$$

Where  $f_{c,t_1}$  = Expected strength at time  $t_1$ , often 28 days

$f_{c,t_2}$  = Estimated strength at time  $t_2$

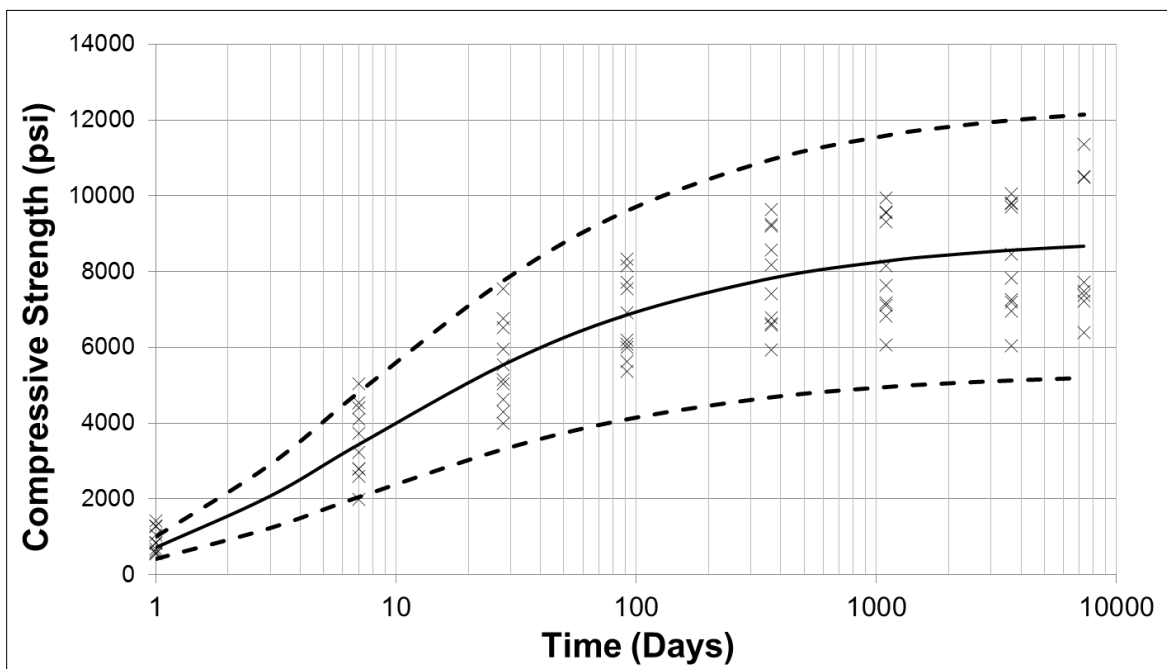
**$s$  = coefficient that depends on the cement type (**



Table E-1-2)

**Table E-1-2 Coefficient,  $s$ , for Various Cement Types**

ASTM Cement Type	$s$
I	0.339
II	0.477
III	0.191
IV	0.739
V	0.553



**Figure E-1-1 Equation E-1-1 for Type II Cement**

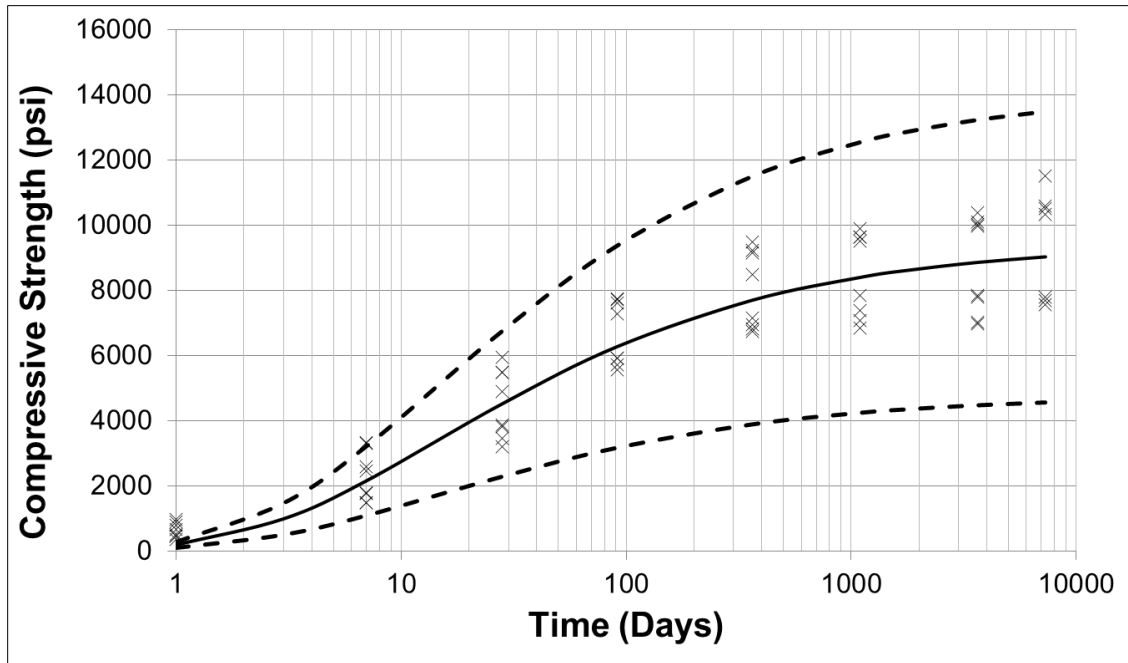


**Figure E-1-2 Equation E-1-1 for Type IV Cement**

**The coefficients presented in**

Table E-1-2 assume the concrete only uses Portland cement concrete. As noted in Section E-1.2.1.3, some mix designs will replace some Portland cement with other cementitious materials. For mass concrete it is common for some of the cement to be replaced by fly ash. This will typically cause a somewhat slower strength gain early on, but a higher gain in strength later in the service life of the structure. Based on the strength gain curves for cement and information on the specified strength and mix design, a reasonable mean compressive strength can be developed for the current age of the structure which can then be correlated to numerous other properties.

#### **E-1.3.1      Strain Rate Effects**

Generally studies have found only a small increase in the compressive strength due to faster strain rates. Most studies have concluded that there is less than a 30% increase with some studies showing virtually no increase (Raphael, 1984) (Min, Yao, & Jiang, 2014). Since the compressive strength rarely controls the strength design or evaluation of mass concrete structures, generally it is acceptable to use the static compressive strength for dynamic analysis. If compressive strength is found to control, a 20% increase is recommended (USBR, 2013). For use in correlations to other properties, the static compressive strength should be used with a dynamic modification for the particular correlated parameter.

#### **E-1.3.2      Sulfate Attack**

Certain sulfate compounds found in some groundwater, soils, and rocks can react with cement to form compounds that have a low solubility and a larger volume than the cement. Due to the larger volume, these reactants will disrupt the concrete and cause extensive cracking in the effected zone. Sulfate attack can occur because of the presence of problematic sulfates in the aggregate or in the water source used in the mix. If this is the case, the corresponding sulfate attack will cause wide spread damage throughout the structure. However, the more common scenario is external sulfate attack, where the reaction takes place due to contact with a sulfate rich material. In this case, the degree to which the concrete will be damaged will be a function of the concrete porosity and how well the sulfate containing water can permeate the structure. Most concrete structures associated with dams and levees will have a low permeability, and if sulfate attack exists it is likely to be localized to the outer surface initially and take many years to penetrate to deeper depths. The affected areas will experience a reduced compressive strength,

and the dimensions of the structure will dictate when the sulfate attack affects the integrity of the structure. As Table E-1-1 implies, if sulfates are known to exist, the concrete mix can be designed to prevent any damage. However, older structures may still be affected by sulfate attack (USBR, 1981) (Zhou, Tian, Sui, Xing, & Han, 2015).

#### **E-1.4 Elastic Properties**

The modulus of elasticity and Poisson's ratio will be needed for linear and non-linear elastic finite element studies. The modulus of elasticity and Poisson's ratio can be determined from uniaxial tension or compression tests if the test specimen was properly instrumented and the data is available from the test (ASTM C469). Again, there are many cases where there is no testing data available and approximations must be made. The modulus of elasticity of concrete has been found to be correlated to the density and the compressive strength. Equation E-1-2 has been adopted by ACI 318 and can be used with the compressive strength calculated using the methods described in Section E-1.3 to estimate the current modulus of elasticity. The unit weight of mass concrete can generally be assumed to be between 150 and 155 pcf, but can be as low as 145 pcf depending on the aggregate used. For conventional concrete with small aggregate, the unit weight is generally near 145 pcf. With the addition of reinforcement, this increases to approximately 150 pcf for normal weight reinforced concrete. For the purposes of Equation E-1-2 the weight of the reinforcement should not be included. Equation E-1-2 is considered applicable to RCC as well as other types of concrete provided the appropriate strength and unit weight are used. The unit weight of RCC will typically be in the same range of 145-155 pcf as conventional mass concrete depending on the degree of compaction.

$$E = 33w_c^{1.5}\sqrt{f_c} \qquad \textbf{Equation E-1-2}$$

Where  $w_c$  = Unit weight of concrete in pcf

$f_c$  = Estimated compressive strength in psi

Poisson's ratio of concrete generally varies between 0.17 and 0.22. Generally a standard value of 0.2 is used for concrete when no test data is available. All types of concrete construction discussed in Section E-1.2.1 will have a similar range of Poisson's ratio.

#### **E-1.4.1      Strain Rate Effects**

Whether the modulus of elasticity is calculated from testing or is correlated from other properties, the rate of loading must be considered. Even if a standard compression test is done slowly enough to simulate a static load, there will still not be enough time for the concrete to creep. These standard laboratory tests are typically referred to as the instantaneous modulus. Therefore if static loading is to be modelled with a linear elastic model, it is common to reduce the instantaneous modulus by 1/3 to estimate the static modulus. Since Equation E-1-2 was developed based on lab test data and, as such, it also does not account for creep in the structure, so the same 1/3 reduction should be applied when using this equation to estimate the modulus of elasticity for static linear elastic analysis. This is a common procedure for concrete gravity structures. For other types of concrete construction, the reduction to account for creep depends on the loading, type of member, and reinforcement. ACI 318 can be used to estimate the effective modulus of elasticity in these cases. For dynamic analysis, some references recommend increasing the modulus obtained from standard tests by 20 to 30% (USACE, 2003). Other investigators have found that the change from the instantaneous modulus is less substantial or non-existent and varies based on numerous other parameters (Malaikah, Al-Saif, & Al-Zaid, 2004) (Mohorovic, Harris, & Dolen, 1999). For this reason it is generally recommended to use the instantaneous modulus for use in dynamic analysis.

Poisson's ratio has also been suggested to be dependent on the strain rate. However, there is no accepted consensus regarding the effect of strain rate on the value of Poisson's ratio, and the data seems to be mixed (Mohorovic, Harris, & Dolen, 1999). For this reason, a value of 0.2 is recommended for static and dynamic Poisson's ratio.

#### **E-1.5    Tensile Strength**

The tensile strength of concrete is an important parameter for the assessment of many concrete structures and is often a key factor discussed during risk analyses of concrete structures. The tensile strength of concrete is a difficult parameter to ascertain and, historically, different testing methods have been used to estimate the tensile strength of concrete. Under ideal conditions the tensile strength is dependent on the strength of the cement, aggregate size, degree of saturation, and rate of loading. In reality there are many other complicating factors. For mass concrete, lift

joints provide a weak plane that will generally have a lower tensile strength than the parent concrete. Even in apparently intact monolithic concrete, cracks will form due to volume and temperature changes. These cracks will relieve stresses in some areas and concentrate stresses in other areas, effectively reducing the gross tensile strength of a given section. There are also numerous methods for testing the tensile strength of concrete, each of which have benefits and shortcomings and will generally give somewhat different results and is why a range of estimated concrete tensile strengths should be considered during a risk analysis. This section will briefly describe these test methods and provide guidance on methods to estimate the tensile strength based on the available test results. In the absence of testing, correlations are also provided.

#### **E-1.5.1 Direct Tension Test**

The direct tension test is the most intuitive method to test the tensile strength of concrete. The test is conducted by affixing the ends of a concrete sample to the load platens of a tension testing machine and failing the sample in uniaxial tension. The tensile strength is then found by dividing the load at failure by the cross-sectional area of the sample. Since the sample is loaded in uniaxial tension, the tensile stress is constant in the axial direction throughout the sample and will therefore fail at the weakest point. If a core from a mass concrete structure is tested that contains a lift joint, the test will simultaneously test the lift joint and the parent concrete with the same axial tensile stress. The test is then able to identify the strength of the controlling area of the sample. The primary downside to this test is that while the test is conceptually simple, it can be difficult to perform successfully in the lab. The drilling to obtain the sample or the shipping of the sample could potentially induce micro-cracks in the face of the sample. Additionally, if the sample is allowed to dry, the corresponding drying shrinkage may also induce micro-cracks in the surface of the sample. Since the sample will be under uniform tension perpendicular to these cracks, the cracks may initiate a tension failure at a load lower than the true tensile capacity of the in situ material. Additionally, if the sample is not placed perfectly vertical in the testing machine, small bending moments will be induced in the sample. These bending moments will increase the tensile stress above the uniaxial value that is intended and will cause the sample to fail prematurely. Both of these effects indicate that the direct tension test will tend to under predict the true tensile capacity of the in situ material. Because of this, if direct tension testing is available it can be considered to represent the lower bound tensile strength.



**Figure E-1-3 Direct Tension Test**

#### **E-1.5.2 Flexure Test**

The flexure test (or modulus of rupture test) is conducted by loading a beam at the third points with two equal loads (ASTM C78). This results in the shear and moment diagrams shown in Figure E-1-4. This shows that within the length of the beam between the two load points, the shear is zero and the moment is therefore constant. If it is assumed that the beam is elastic and the displacements are small up until the point of failure, then the tensile stress present at the bottom of the beam can be determined from the magnitude of the point load. Provided that the beam was proportioned such that it fails in moment rather than shear, at the point of failure, the modulus of rupture can be calculated using Equation E-1-3. An example of this test being conducted is shown in Figure E-1-5.



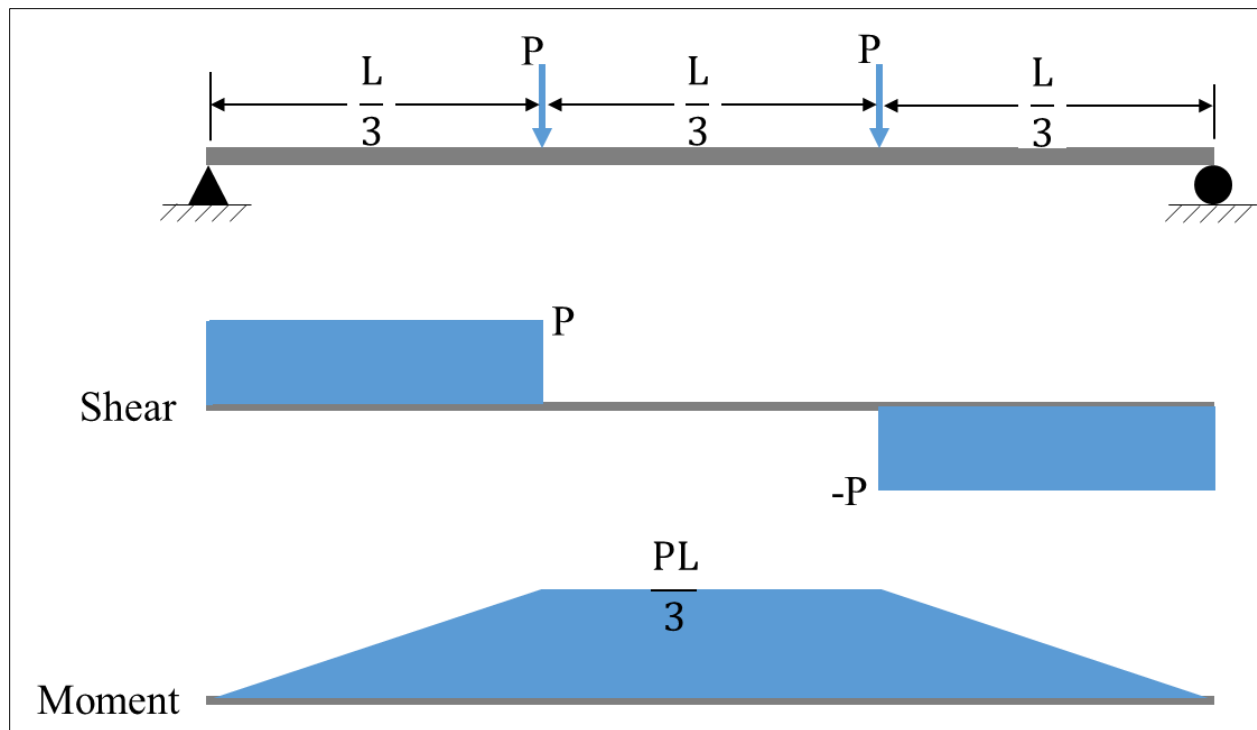


**Figure E-1-4 Flexure Test Shear and Moment Diagrams**

$$f_r = \frac{PLd}{6I}$$

**Equation E-1-3**

Where  $P$  = Load on beam at failure

$d$  = Depth of the beam

$I$  = Moment of inertia of the cross-section

$L$  = Length of beam



**Figure E-1-5 Concrete Flexure Test**

As noted above, Equation E-1-3 assumes that the material is linear elastic. At this point it is instructive to look at the stress-strain diagram for the direct tension test. Figure E-1-6 shows an example stress-strain curve in blue which indicates that concrete is only approximately linear elastic at low stresses and then deforms plastically as it approaches failure. The direct tension strength will be the peak stress obtained on the curve, which is slightly higher than the stress at failure. Because the flexure test calculates the stress at the point of failure assuming a linear elastic stress, the calculated tensile strength will be significantly higher than the direct tension strength because it neglects the plastic strain in the concrete near failure. Because this stress does not represent the true tensile strength of the material, it is commonly referred to as the modulus of rupture. Depending on the application, this may not be a shortcoming of the test. For example, if the initiation of cracking of a concrete structure needs to be identified from a linear elastic finite element model, then the critical stress should be the modulus of rupture rather than the true direct tension strength. This is because the linear numerical model will not allow the material to deform plastically, so in order to obtain a strain equal to the true failure strain, the modulus of rupture must be used as the stress criteria.

Figure E-1-5 depicts a rectangular section. This section was cast as a beam. However, Equation E-1-3 can be used for a circular cross-section as well by using the appropriate moment of inertia. This means that a drilled core can be used for this test as well. Since the test results in a zone of constant moment in the middle third, the test is also capable of identifying the weak point in this zone. Therefore, if the core contains a lift joint, the sample can be cut such that the lift joint falls within the middle third, and the test will effectively test the modulus of rupture of the lift joint as well as the parent concrete.

To summarize, the benefits of the flexure test are that the modulus of rupture can be directly measured for parent concrete and lift joints of core samples which can then be used directly in linear elastic finite element models. The shortcomings of the test are that, similar to the direct tension test, the results will be sensitive to cracking on the tension side of the sample from drying of the sample or cracking during the drilling or shipping process. Additionally, the sample must be three times longer than the diameter to ensure a flexure failure. For large core diameters this may require a high core recovery, which may be difficult to achieve.

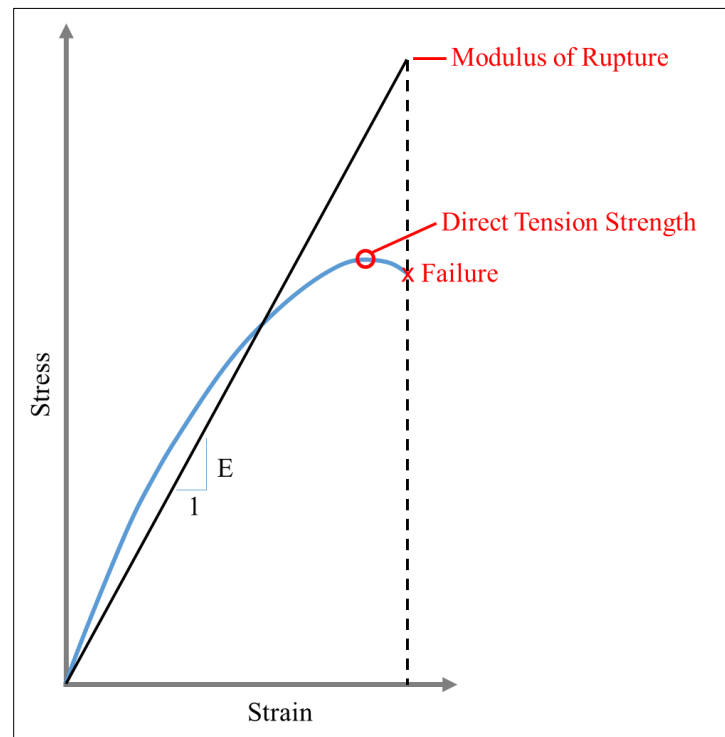


**Figure E-1-6 Stress-Strain Diagram for Direct Tension Test**

### **E-1.5.3      Splitting Tension Test**

The splitting tension test (also referred to as the Brazilian Test) is one of the most commonly performed due to its simplicity. The test is conducted by loading a concrete cylinder in compression along a strip on its circumference as shown in Figure E-1-7. Loading the cylinder in this way can be idealized as loading a circular cross-section by two equal and opposite point loads along a diameter of the circle. This results in a radial distribution of compressive stresses that emanate from each of the point loads. Superimposed on these two radial stress distributions is a uniform tension of magnitude  $\frac{2P}{\pi dL}$  throughout the plane of the circular cross-section, where  $P$  is the magnitude of the applied force on the cylinder,  $d$  is the diameter of the circle, and  $L$  is the length of the cylinder (Timoshenko & Goodier, 1951). When these stress distributions are added together, the maximum principle stress distribution shown in Figure E-1-8 results. As can be seen, this results in a relatively uniform zone of tension perpendicular to the diameter between the two point loads. When the tensile stress at the center of the circle reaches the tensile capacity of the concrete, the cylinder will split along this diameter. Thus, the splitting tensile strength can be found using Equation E-1-4 using the load applied to the cylinder at the time of failure.



**Figure E-1-7 Example Splitting Tension Test**

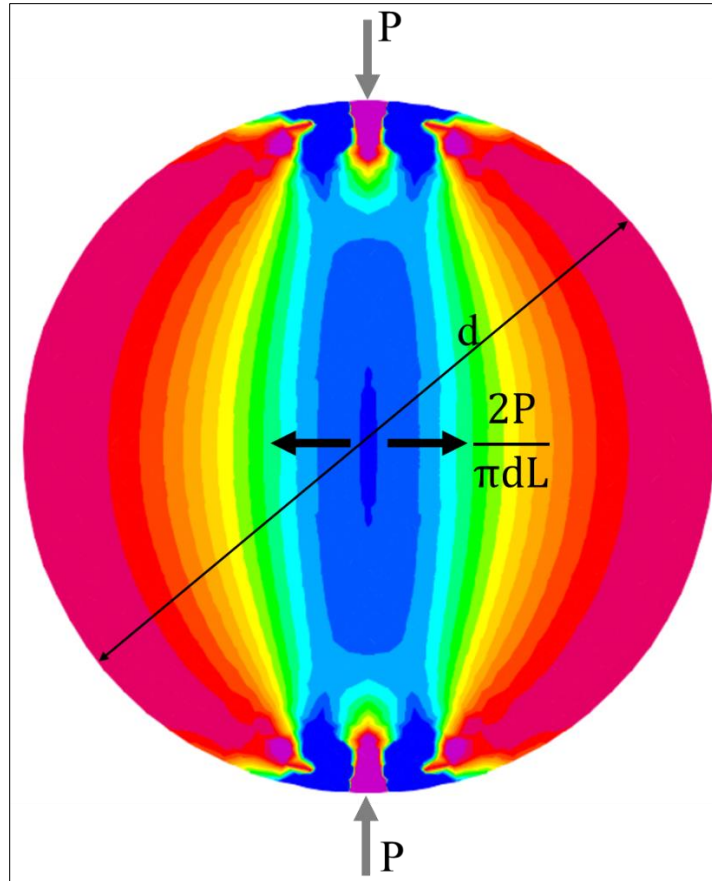


**Figure E-1-8 Maximum Principle Stresses during Splitting Tension Test**

$$\sigma_t = \frac{2P}{\pi dL}$$

**Equation E-1-4**

Where P = load at failure

d = Sample diameter

L = Sample Length

The theoretical stress distribution is based on the applied load being in the form of two point loads. These point loads will in theory produce singularities of infinite stress at the point of application, which would tend to locally fail the concrete at the face of the cylinder.

Additionally, the zone of uniform tensile stress near the center of the cylinder must be developed along the entire length of the cylinder as uniformly as possible. This requires that the compressive load on the cylinder is applied uniformly along its length. To achieve this and to spread out the load at the point of application, ASTM C496 requires that ¼ inch thick and 1 inch

wide wooden bearing strips are used to distribute the loading from the steel bearing bar or plate. These bearing strips help to distribute the load along the length of the cylinder and also distribute the load on the circular cross-section. With the load distributed, there is sufficient confinement to prevent localized failure from the high compression stresses at the point of load application.

The splitting tension test is a relatively inexpensive test because it is simple to perform and can easily be performed on cast cylinders or drilled cores. The test is also insensitive to micro fractures from the drilling process or from drying shrinkage since these cracks would most likely occur at the face of the cylinder, which is in compression at the location of the failure plane. However, there are also numerous drawbacks to the method. First, because of the stress distribution in Figure E-1-8, the tensile failure of the specimen is forced through the plane between the load points. This failure plane may go through large pieces of aggregate, and will generally not be the weakest plane through the concrete. This effect will be exacerbated if the sample is not large enough relative to the nominal maximum aggregate size. This effect of forcing the failure plane through the center of the core is especially problematic for cores taken from a mass concrete dam. In most cases it is convenient to drill through the dam vertically or at a steep angle to obtain core samples. Since the lift joints in the concrete are horizontal, this means that in the sample tested in the lab, the lift joint will be perpendicular to the failure plane, and the splitting tension test will be testing the parent concrete, not the lift joint. Since the lift joint is very likely the weak plane in the concrete, the tensile strength on this plane is often the critical location that needs to be tested. This will be difficult using the splitting tension test unless the core is drilled horizontally through the concrete with such precision that the lift joint is located at the center of the core, which is typically impractical.

The second issue with the splitting tension test involves the confinement provided by the wooden bearing strips. It has been suggested that the confinement provided by the strips may delay the development of the tension failure from what would have occurred in the theoretical case using Equation E-1-4 that assumes point loads (Rocco, Guinea, Planas, & Elices, 1999). This effect has been illustrated by testing a pre-split core shown in Figure E-1-9. This test shows significant strength of the core due to the confinement of the bearing strips (Dolen, Harris, & Nuss, 2014) and resulting distribution of the applied load to the two halves of the split core. This pre-split test



can only be interpreted as an illustration of the bearing strip effect. Specifically, since the sample is already cut, the stress distribution throughout the sample is completely different than for an intact sample and can in no way be considered a tension test and in no way disproves the benefit of performing a splitting tension test. Rocco et al (1999) found that this effect can be adequately reduced by having a large ratio between the size of the sample and the size of the bearing strip.



**Figure E-1-9 Splitting Tension Test of a Pre-Split Sample**

Lastly, Equation E-1-4 assumes that the sample is behaving elastically. As Figure E-1-6 illustrates, this is not a valid assumption and results in higher predicted tensile stress for the modulus of rupture test. Though this effect is may be smaller for the splitting tension test, it likely contributes to the overestimation of tensile strength by the splitting tension test.

#### **E-1.5.4 Correlations**

The above discussion can be used to help interpret existing test results or to develop a testing program for a project. In many cases it may be necessary to perform analysis without any tension testing results. In these cases correlations are available to estimate the tensile strength from the

compressive strength. The most comprehensive effort to date to develop a correlation between compressive strength and tensile strength was conducted by Jerome Raphael (1984) who examined approximately 12,000 individual test results containing a combination of primarily splitting tension and flexure testing with a small number of direct tension testing. Raphael then developed Equation E-1-5 to estimate the splitting tension strength from the compressive strength. Based on the flexure tests, Raphael found that the modulus of rupture was approximately 1.35 times the splitting tension test. ACI 318 gives Equation E-1-6 for the modulus of rupture and states that the splitting tension test is approximately 90% of this. Cannon (1995) subsequently did an in depth evaluation of concrete tensile strength for conventional mass concrete and RCC using Raphael's and ACI's equations as a starting point. First, Cannon noted that the Raphael equation slightly over predicts tensile strength at low compressive strength, while the ACI equation more significantly over predicts the tensile strength in this range. Both equations were found to be satisfactory for compressive strengths greater than 3500 psi. Therefore, Cannon confirmed that Raphael's equation based on splitting tension strength is appropriate, but recommended several adjustments for factors not considered directly by Raphael. The majority of Raphael's data was based on testing of concrete with relatively small aggregate. Mass concrete typically has larger aggregate to reduce volume changes during the curing process. To account for large aggregate (> 1.5 inches) Cannon recommended a 10% reduction from the splitting tension strength predicted by Equation E-1-5. As discussed above, splitting tension strength is expected to give a higher strength than direct tension even if both tests are conducted perfectly. If the direct tensile strength is desired, Cannon recommended a reduction of 20% from the splitting tension strength predicted by Equation E-1-5. Cannon also concluded that if RCC is mixed to be sufficiently workable, it will have tensile strengths approaching that of conventional mass concrete with strengths of 0.73 to 1.06 times that of conventional mass concrete.

A comparison of the data that Raphael used to determine his correlation with additional data compiled by Cannon with Raphael's correlation (Equation E-1-5) and the ACI correlation for splitting tension (90% of Equation E-1-6) is shown in Figure E-1-10. This illustrates that the ACI equation over predicts the tensile strength at low compressive strengths, but both correlations fit the data reasonably well at higher strengths. Also shown in the figure is Raphael's equation



corrected for large aggregate, direct tension, and lift joints, which shows a reduction in the static strength, approaching 5% of the compressive strength.

$$\sigma_t = 1.7f_c^{2/3}$$

**Equation E-1-5**

$$f_r = 7.5\sqrt{f_c}$$

**Equation E-1-6**

Where  $f_c$  = Estimated Compressive Strength

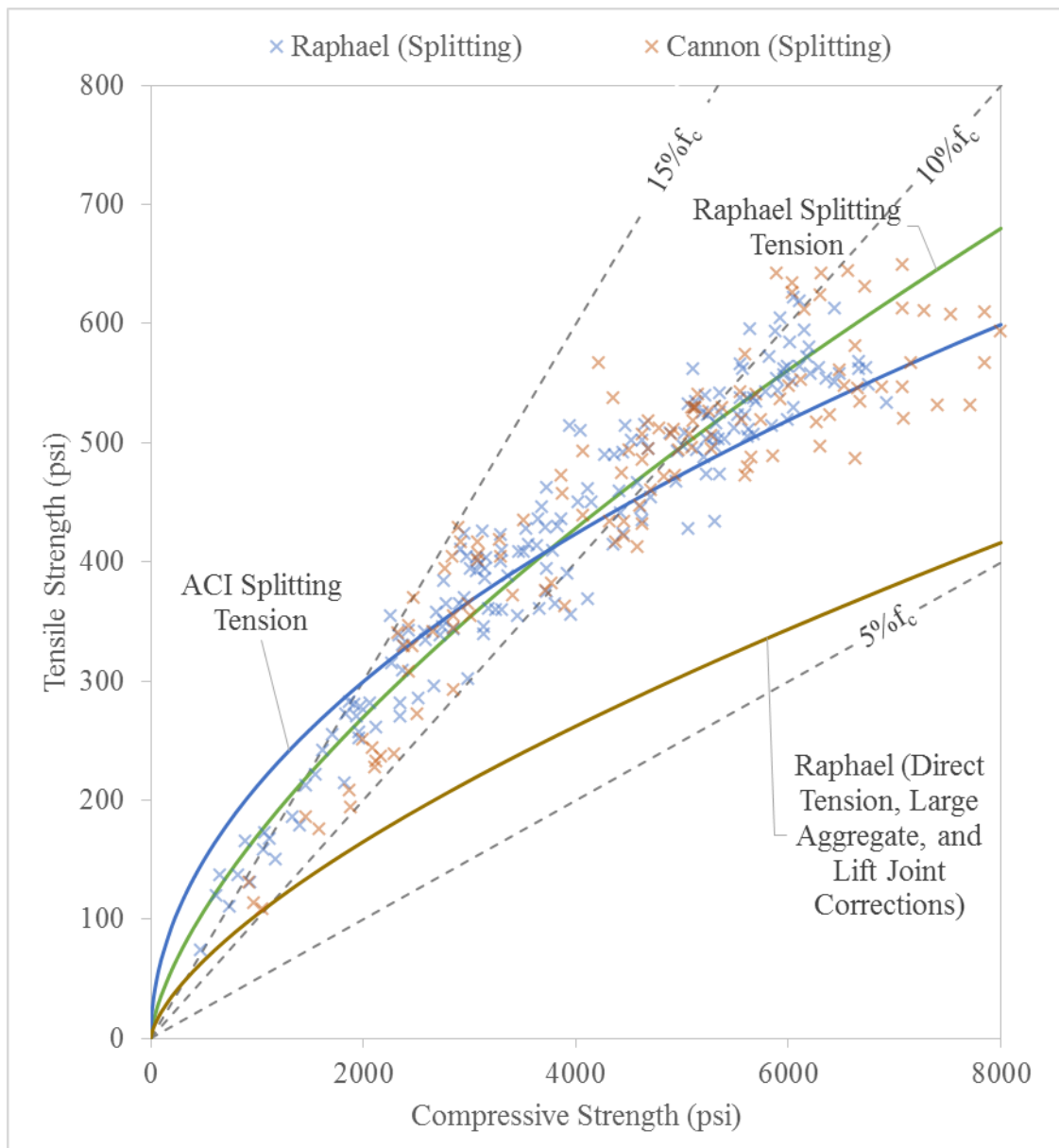


**Figure E-1-10 Comparison of Tensile Strength Correlations with Available Data**

#### **E-1.5.5 Strain Rate Effects**

The rate of loading is an important parameter for the tensile strength of concrete. Raphael also investigated this effect using data from six western dams loaded to the maximum value in 0.05 seconds and found an average increase from the static strength of 66% for direct tension results and 46% for splitting tension tests. Based on these results, a 50% increase for dynamic loading was recommended. Other studies have also found a 50% increase in dynamic strength at relatively high strain rates including the Cannon (1995) study. However, most of these studies evaluated monotonic dynamic loading of moist or saturated concrete. Saucier (1977) is one of

the few studies that investigated both wet and dry samples and the effect of repeated dynamic loading. This study found that there was an increase in the monotonic dynamic tensile strength of concrete if the samples were wet. There was no increase observed for dry samples. This means that the dynamic increase in concrete strength is likely at least partly due to the development of negative pore water pressures in the concrete that resist the tensile forces. It is likely that the concrete does not need to be completely saturated to develop some dynamic increase. In most dam and levee concrete structures where earthquake loading is a risk driving failure mode, it is likely a reasonable assumption that the concrete has a sufficient water content to develop increased strength under rapid loading. However, in cases where the concrete is known to have a low moisture content it may not be appropriate to increase the strength significantly from the static strength.

As concrete approaches its tensile strength micro-cracks will tend to form that result in the non-linear deformation shown in Figure E-1-6. If a sample is loaded to a stress somewhat less than its tensile strength, some damage is done to the concrete. If the concrete is then cycled through another identical load, the cracks will propagate further. This damage to the concrete will tend to lower the strength of the concrete. Thus, the concrete should fail at lower stresses if it experiences more cycles. And similarly, the concrete will sustain fewer cycles if it is cycled to higher stresses. Furthermore, there is some stress where the concrete remains essentially elastic and can withstand an unlimited number of cycles. Consistent with these general concepts, Saucier (1977) found that no specimens failed when cycled to 60% of the estimated strength and 24% failed when cycled to 80% of the estimated strength. The cyclic fatigue testing was only conducted on dry samples, meaning that the estimated tensile strength was near the static strength of the concrete. However, it is reasonable to expect cyclic fatigue effects of wet concrete as well since the development of micro-cracks would reduce the ability of negative pore pressures to develop.

#### **E-1.5.6      Lift Joint Strength**

Lift joints represent a weak point in a mass concrete and RCC structures and will therefore generally control the response of mass concrete structures. Compounding this issue, due to ease of construction and formwork placement, it is common for lift joints to be located at or near

changes in geometry, which will develop stress concentrations. For this reason, it is important to establish the strength of the lift joints. As noted above, the lift joint strength can be directly measured if cores can be taken that contain a lift joint. When site specific data is lacking, the concrete placement practices should be reviewed. The methods for placing lifts of concrete differ between conventional mass concrete and RCC.

#### **E-1.5.6.1 Conventional Mass Concrete**

Good lift joint cleanup of conventional mass concrete consists of removing any laitance or otherwise poor concrete at the surface of the lift and exposing the aggregate of the lift joint without undercutting the aggregate. This can be accomplished with green cutting or high pressure water jetting. The joint then should be allowed to dry such that there is not standing water on the surface prior to the next placement of concrete. These practices will ensure quality concrete at the lift joint, aggregate interlock between lifts, and will promote a good bond with the next lift. Concrete placement practices should include a low water-to-cementitious material ratio to prevent bleeding at the joint and development of laitance, a rich mix with smaller aggregate adjacent to the joint, and good concrete layering and vibration. In older dam construction mortar was sometimes placed between lifts to promote a good bond. However, in many cases this has been found to reduce the strength of the joint and has been abandoned in more recent mass concrete construction. These practices are depicted in Figure E-1-11.

It is often difficult to assess from visual inspection whether the lift joints are bonded or not. For example, the amount of leakage seen on the downstream face along the lift joints has at times been used to determine the likelihood of bond. Seepage on the downstream face of a concrete dam is not a reliable indicator of lift joint bond. Friant Dam has many large seeps on the downstream face along the lift lines but extracted cores indicated bonded lift surfaces. Based on the cores, it appeared that the bottom of the concrete lifts were not consolidated as well and were more porous than the overlying concrete, forming a seepage pathway. Though a seepage pathway was formed, there was found to be enough paste at the bottom of the lift to bond to the underlying lift. In contrast, Stewart Mountain Dam has a dry downstream face, but extracted core showed 16 of 23 lift joints unbonded. Failure to thoroughly clean the laitance from the lift surfaces resulted in weak bond, but there were sufficient fine particles at the interface to limit

seepage along the joint. Therefore, it is important to locate as much information as possible about the methods and specific conditions encountered during construction, which are often keys to the strength of lift joints.

If good construction practices and quality control occurred during construction, the lift joint strength can approach the strength of the parent concrete. In laboratory tests of lift placement techniques it has been found that if the top of the previous lift is wet when the next lift is placed, the strength of the lift joint is on average 72% of the parent concrete strength. If the previous lift was allowed to dry before placing the next lift, the lift joint strength was 82% of the parent concrete strength (Tynes & McCleese, 1973). In the field, lift joints at Hoover Dam have been found to be approximately 92% of the parent concrete strength. Where poor lift joint practices exist, low tensile strengths can exist. In the worst case, a bond will not be formed between lifts and the tensile strength will be zero.



**Figure E-1-11 Good Joint Cleanup and Concrete Placement Practices**

#### **E-1.5.6.2 Roller Compacted Concrete**

Unlike conventional mass concrete which may be placed in lifts 5 ft in height or greater, RCC must be placed in short lifts of 6 to 24 inches in order to fully compact each lift. This introduces

more planes of weakness into the structure when compared to conventional mass concrete. Each lift is compacted with a vibratory roller which tends to orient the long side of any aggregate in the horizontal direction which can reduce the interlock of the aggregate across the joint and reduce the bond and sliding strength. Unlike conventional mass concrete where adding a mortar layer at the lift joints was not found to improve the bond, this has been shown to improve the lift joint bond of RCC. Where the RCC has been adequately compacted, the lift surface has been adequately prepared and the RCC is placed prior to formation of a cold joint the strength of the lift joint can be expected to be between 70 and 75% of the parent concrete strength. To achieve similar strengths for cold joints, bedding mortar is placed between the lifts. However, the bond strength is sensitive to the aggregate size, degree of compaction, and use of mortar bedding. These factors should be evaluated when estimating the bond strength.

#### **E-1.5.7      Alkali Aggregate Reaction**

In some cases an aggregate may have been chosen for a concrete mix that is incompatible with the alkali hydroxides in the cement. In these cases there will be a reaction between the minerals in the aggregate and the cement which cause expansion and cracking of the concrete. The most common form of alkali aggregate reaction is alkali silica reaction (ASR) in which silica minerals in the aggregate react with the cement. This results in a gel formed from the reactants that surrounds the problematic aggregates and will absorb water. As the water is absorbed the gel swells and causes the characteristic concrete growth. This gel also has essentially no tensile strength and can therefore create a plane of weakness as more and more aggregate is affected. The effect on compressive strength and modulus is less of a concern, but this must be considered when evaluating the tensile capacity when it is found to exist at a project. The other less common form of alkali aggregate reaction is alkali carbonate reaction (ACR) which is caused by the breakdown of dolomite in the concrete, and therefore only occurs with dolomitic aggregate. The chemical reactions associated with the breakdown of the dolomite is usually accompanied by expansion, and therefore has similar effects as ASR. ACR is responsible for induced stresses, joint misalignment, and reduced strength and stiffness at Chickamauga Locks and dam on the Tennessee River.

#### **E-1.5.8 Sulfate Attack**

Similarly to compressive strength, sulfate attack will significantly degrade the tensile strength of concrete, but only in the affected area which is likely to be the outer faces of the structure. The outside faces will also generally be the location of the highest tensile stresses. These areas of reduced tensile strengths should be considered in the evaluation of affected structures.

#### **E-1.5.9 Best Practices in Estimating Tensile Strength**

Once the available site information has been reviewed, it will likely be necessary to make some modification to the available information to develop a reasonable estimate of tensile strength for use in analysis. In all cases, the best site specific information should be used. In the worst case scenario where there is no tensile strength testing data available for the site, Equation E-1-5 can be used to estimate the static splitting tensile strength of the parent concrete, assuming small aggregate, based on the estimated compressive strength. Given this, Table E-1-3 can be used to adjust this strength as necessary. The table can also be used in reverse if needed by dividing by the indicated factor to get from the “to” column to the “from” column. It should be noted that the apparent linear strength is the same as the modulus of rupture and the non-linear strength is the same as the direct tension strength, thus  $1/1.33$  is approximately 0.75. The table was created with some duplicate information for ease of use. This table is primarily intended for conventional mass concrete and conventional reinforced concrete. For RCC, consideration must be given to other items discussed in the previous sections, such as degree of compaction, aggregate size and shape, mortar bedding, lift size, etc.

**Table E-1-3 Summary of Correction Factors**

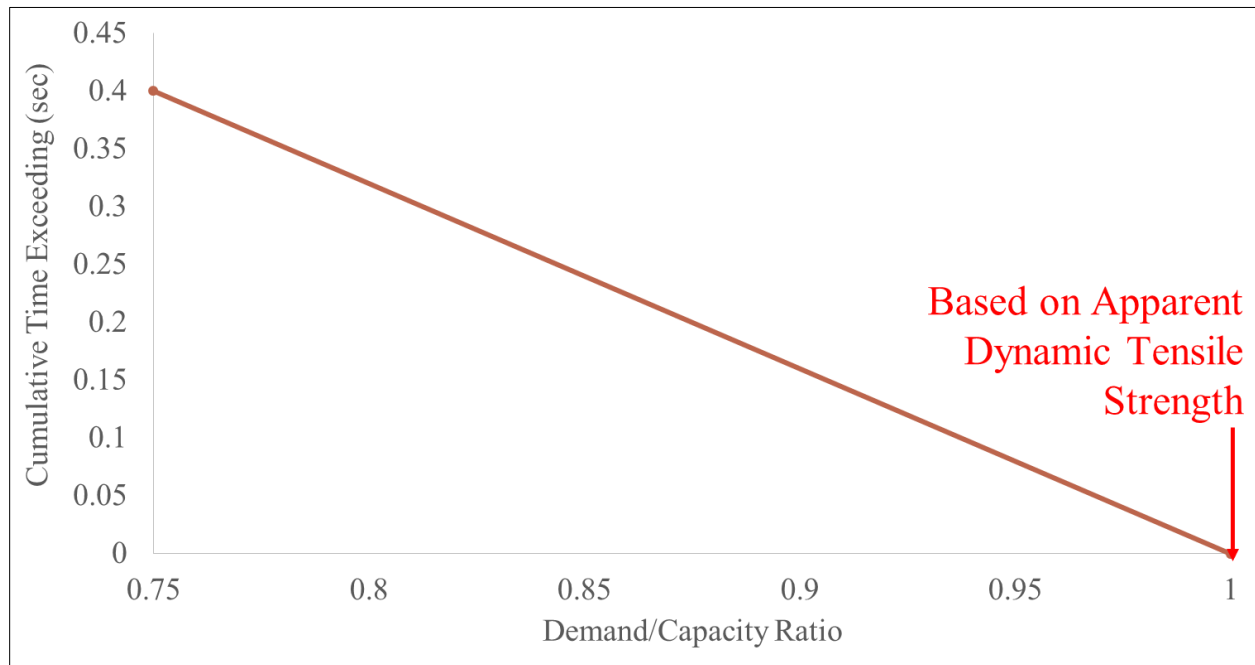
Correct from:	To:	Multiply by:
Splitting Tension	Direct Tension	0.8
Modulus of Rupture	Direct Tension	0.75
Small Aggregate	Large Aggregate	0.9
Parent Concrete	Well Prepared Lift Joint	0.85
Static Loading	Rapid Loading	1.5
Nonlinear Strength	Apparent Linear Strength	1.33

Table E-1-3 gives the maximum static and dynamic tensile strength. However, when evaluating dynamic analysis results for tensile capacity, the effect of cyclic fatigue as described above must also be considered. If the maximum tensile stresses in a model are generally below 75% of the estimated dynamic tensile strength then cracking should be minimal. In cases where the full dynamic tensile strength is exceeded over 20% of a given cross-section, the cracking will likely be extensive. In between these cases, the duration of time above the tensile strength must be considered. The concept of a concrete performance curve for this purpose was developed by Ghanaat (2002) and was subsequently adopted by in EM 1110-2-6051 (USACE, 2003). A similar performance curve is given in Figure E-1-12 modified slightly to incorporate the information summarized in the preceding portion of this chapter. This curve allows for 75% of the dynamic modulus of rupture to be exceeded for a total of 0.4 seconds, whereas it is not allowed to exceed the full dynamic modulus of rupture at all. This curve can be used along with the spatial distribution of the high stresses to decide if a more rigorous non-linear analysis is warranted.

Section E-1.7 provides two potential material models for non-linear finite element models. These models make assumptions about the concrete properties. For example, a dynamic strength



enhancement curve is provided for one material model (Figure E-1-16). This indicates a significantly higher tensile strength enhancement for some strain rates than recommended above. Some testing of the material models is therefore warranted to ensure that reasonable tensile strengths are used at the strain rates of interest.



**Figure E-1-12 Mass Concrete Performance Curve for Linear Elastic Analysis**

### **E-1.6 Shear Strength**

There are two types of shear strength failures that are generally seen in concrete structures. For monolithic concrete members with a relatively short dimension in the direction of the shear force, a diagonal tension failure is observed. This failure is caused by the shear forces, but the material itself does not fail in shear. This type of failure is common in reinforced concrete members, and the capacity for this type of failure is generally found to be a function of the square root of the concrete compressive strength. Equations and guidance for evaluating this type of failure can be found in ACI 318, EM 1110-2-6053, other concrete design codes, and the Reinforced Concrete Chapter of this manual (Chapter E-2). For mass concrete structures, shear failures are generally better approximated using Mohr-Coulomb shear strength criterion. This is because in mass concrete structures the cross-sections are generally very large with preferential shear failure planes at the lift joints, which cause a pure shear failure to control. Additionally, tensile cracking will often precede a shear failure, further reducing the strength of the

preferential shear planes at the lift joints. The shear strength of the concrete can be measured in the lab using a direct shear machine. Because mass concrete is typically evaluated at a predefined plane, the triaxial shear strength is typically not appropriate. Direct shear testing can be used to assess the intact shear strength along a predefined plane and the sliding strength along an unbonded sample. Care must be taken when evaluating the lab results from direct shear testing to ensure that shear strength parameters are developed based on the stress range of interest for the structure in question and the expected loading. It is generally convenient to assume that the shear failure envelope is linear, when in fact if a large enough stress range is tested, it will be found that the envelope is non-linear. If a straight line is fit to test data over a wide range of stresses, the straight line will inevitably show an apparent cohesion intercept, even for an unbonded sample. Figure E-1-13 shows that this cohesion is artificial when the actual non-linear failure envelope is considered. The apparent cohesion would be appropriate if the range of stresses in the structure are in the middle range of the figure. However, gravity structures often have low normal stresses, and the straight line fit can overestimate the shear strength in this zone, shown with the blue shaded region in Figure E-1-13.

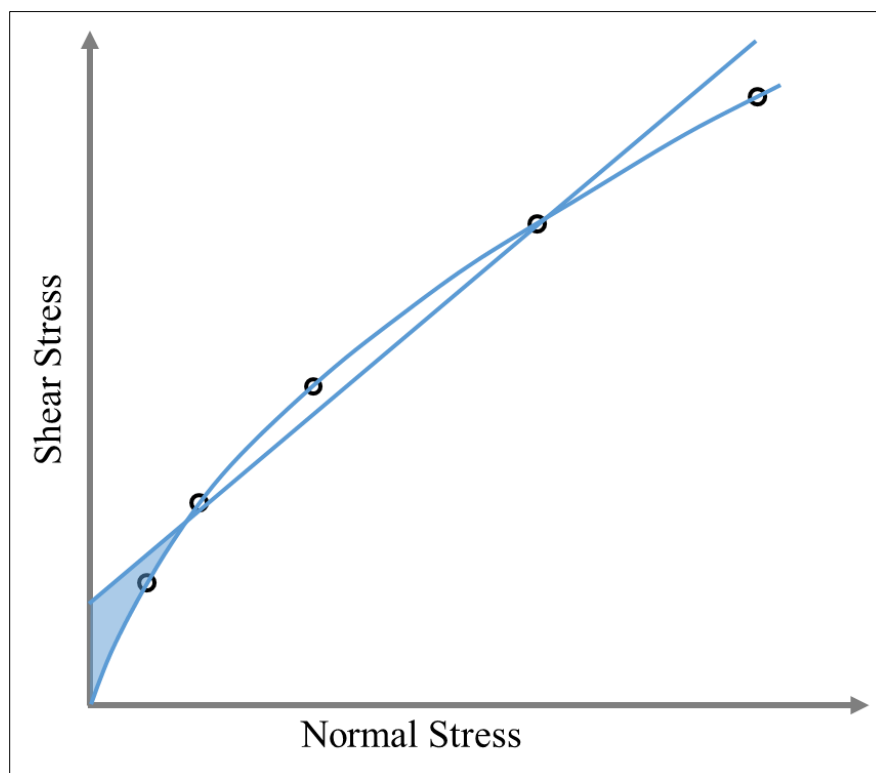


**Figure E-1-13 Example Direct Shear Lab Data**

In the absence of site specific shear strength data, bonded and unbonded shear strength parameters can be estimated from compiled data from many dams published by the Electric Power Research Institute and reproduced in Figure E-1-14 (Stone and Webster Engineering Corporation, 1992).

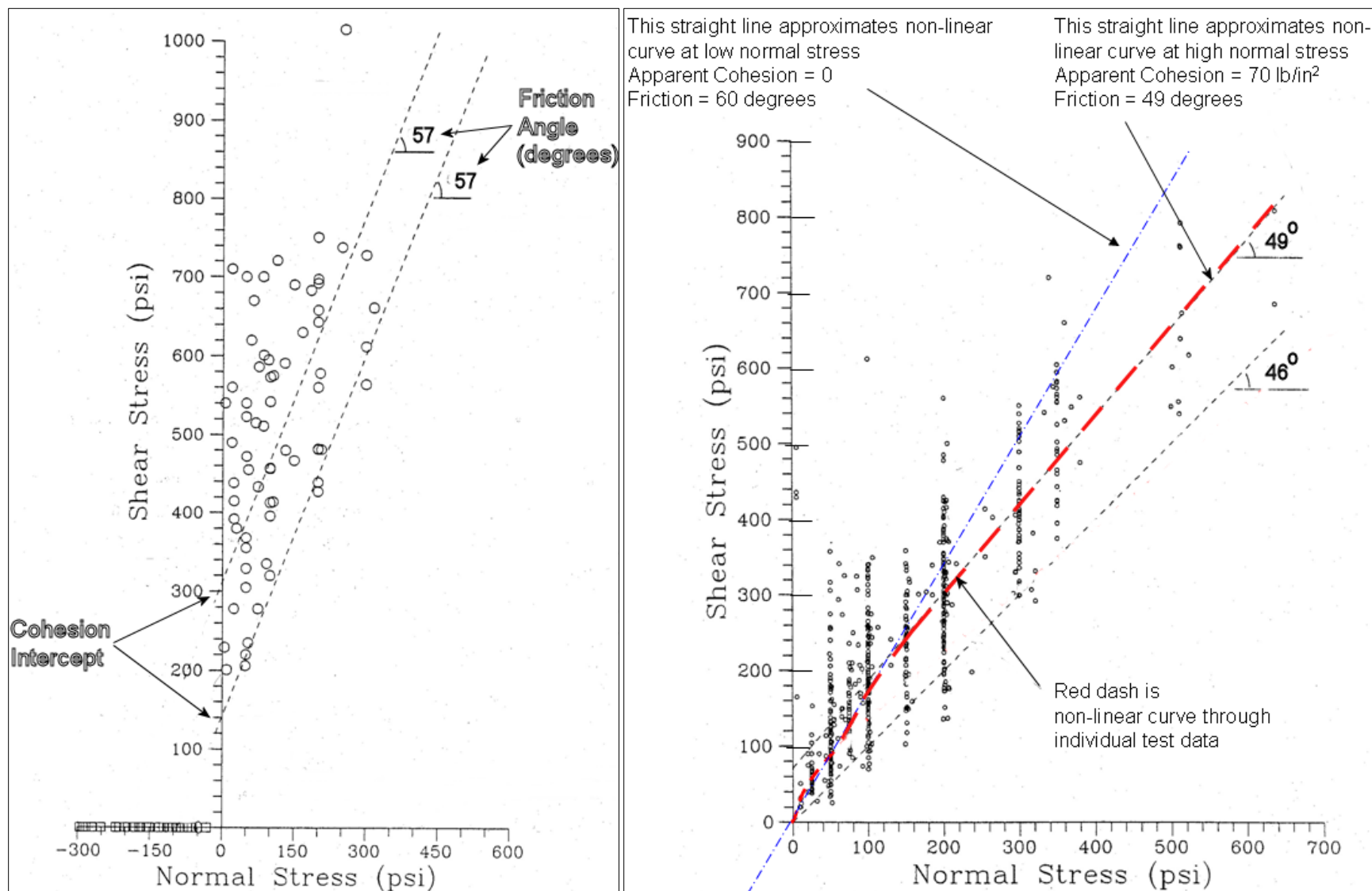


**Figure E-1-14 Bonded (Left) and Unbonded (Right) Shear Strength Parameters**

Figure E-1-14 gives a compilation of shear strength data for both bonded and unbonded lift joints. The bonded shear strengths are characterized by a high friction angle and cohesion. The unbonded strengths cover a wide range of normal stresses and therefore show some amount of non-linearity. Therefore Figure E-1-14 recommends a bilinear shear strength envelope with a higher friction angle and zero cohesion at low normal stress with a lower friction angle and apparent cohesion at higher normal stress. All of the samples used to develop Figure E-1-14 are based on conventional mass concrete. A comparable dataset for RCC dams is not available. For RCC construction consideration should be given to degree of compaction, aggregate size and shape, mortar bedding, and lift size when determining the shear strength parameters.

In many cases, if a lift joint is sampled it may be found that the joint is not fully bonded, but has areas with bond and others without. When analyzing these cases, the strain compatibility between the bonded and unbonded areas must be considered. Figure E-1-15 shows a schematic comparison of the shear stress vs displacement diagram for bonded and unbonded samples. The bonded sample is shown to be much stiffer than the unbonded sample. On a failure plane with bonded and unbonded portions, the bonded portions will attract much more load than the unbonded portions due to the difference in stiffness. This means that the two peak strengths are not additive. Generally the amount of load that the unbonded portion attracts is so minor that the bonded portion can be considered to take all of the load until failure, at which point the entire failure plane becomes unbonded.

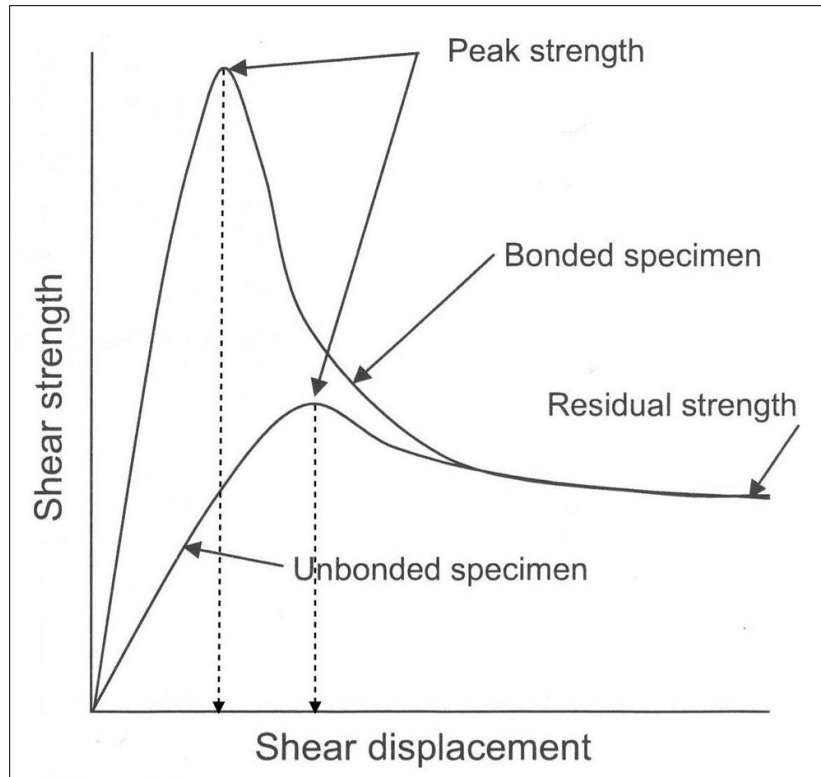


**Figure E-1-15 Shear Displacement vs Shear Stress for Bonded and Unbonded Concrete Joints**

#### **E-1.6.1 Strain Rate Effects**

There is less research on the change in shear strength of concrete with dynamic loading than other concrete properties. There is likely an increase in the shear strength under dynamic loading, particular for bonded joints due to the buildup of negative pore pressures. The effect on unbonded joints is probably much smaller. Where this has been studied in rock joints the effect has been found to be minimal (Scott, 1982). While research continues in this area, the current practice is to use the static strengths for static and dynamic analyses.

#### **E-1.6.2 Alkali Aggregate Reaction and Sulfate Attack**

Both alkali aggregate reaction and sulfate attack will likely have some deleterious effect on the shear strength of concrete. However, alkali aggregate reaction will also cause significant growth of the concrete which also has the potential to increase the confinement of the structure, which may offset the reduced shear strength caused by the gel formed around the aggregate. Sulfate attack will also reduce the shear strength in the affected area. But since the affected area may be fairly limited relative to the cross-section of a mass concrete structure, it may not significantly

affect performance depending on the type and progression of the sulfate attack and the dimensions of the structure.

### **E-1.7 Using Concrete Properties for Finite Element Analyses**

The information discussed above can be implemented in finite element analyses in order to evaluate nonlinear behavior of structures. This section will provide some guidance on how to do this and will present some verification studies. Two concrete material models will be compared, namely:

- 1) The Karagozian & Case concrete model, release III (KCIII). This model is a three-invariant model and uses three shear failure surfaces, including damage and strain rate effects. The damage is displayed on a scale from zero to two (two showing the element completely cracked or crushed.) This model has parameter generation capacity based solely on the unconfined compression strength of the concrete, which will be used here (Livermore Software Technology Corporation, 2012).
- 2) The Winfrith Concrete model (BNW). This model was developed by Broadhouse and Neilson over many years and has been validated against experiments. Rebar may be included using the smeared rebar approach or by the use of discrete rebar beam elements (Livermore Software Technology Corporation, 2012).

First, the behavior of a column in tension and compression was considered. The column was unreinforced in order to illustrate the tension and compression behavior of these two materials and was proportioned to preclude buckling. Displacement control was used, since any failure is expected to be sudden.

Next, a simply supported concrete beam with reinforcement was studied. This beam was subjected to a uniform load producing bending; flexural capacity was compared to classical solutions.

#### **E-1.7.1 Column Behavior**

The following material inputs are used for the two concrete models: (critical input parameters are discussed and can be obtained from methods discussed previously, while all others are default values recommended for the material model)

### Inputs for Material KCIII:

- Concrete mass density = 0.00022 slugs (146.9 lbs/ft<sup>3</sup>)
- Poisson's ratio = 0.18
- Concrete cracking capacity = 500 psi (static direct tensile strength)
- Concrete compression strength = -5000 psi (negative sign tells the material model to generate all typical input parameters)
- Effective strain rate vs strength enhancement curve. A suggested curve developed by Karagorzian & Case and the Naval Facilities Engineering Service Center is plotted in Figure E-1-16 and can be used in lieu of tested values. Since the material model is defined by 3 shear failure surfaces, the strength enhancement is technically a shear strength enhancement, but will affect the tensile and compressive strength depending on the loading (Malvar & Crawford, 1998).

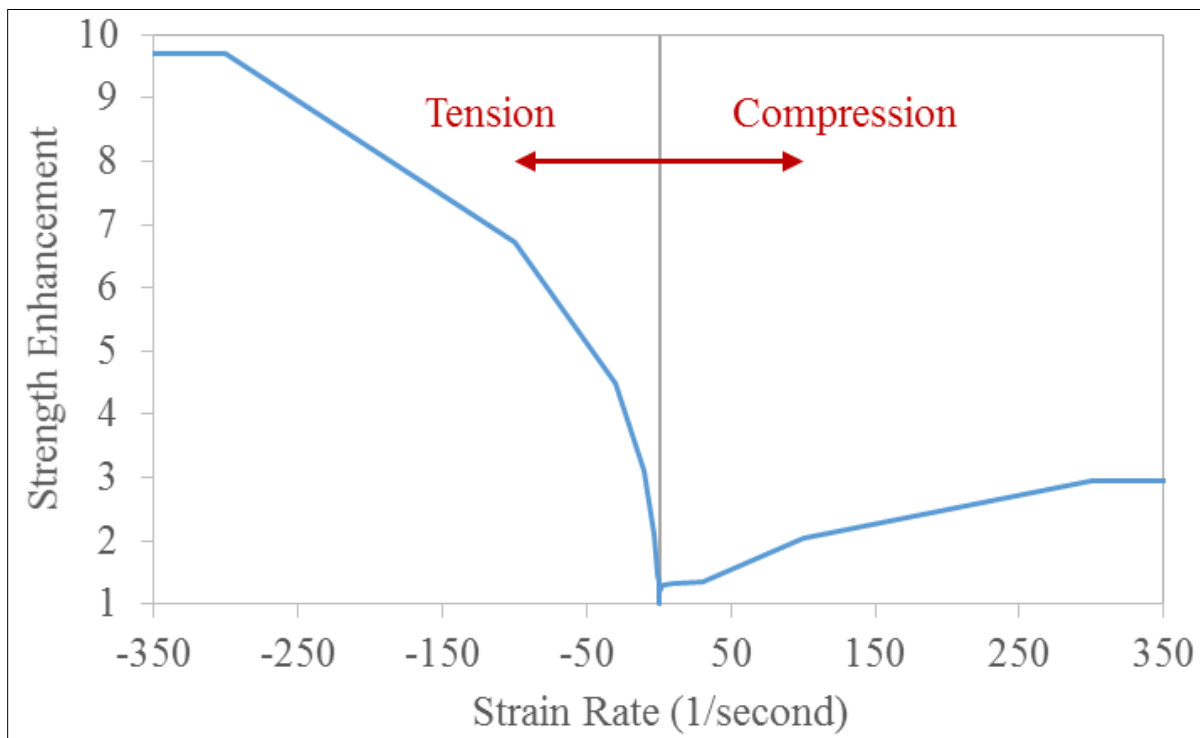


**Figure E-1-16 Strain Rate Dependent Strength Enhancement**



Inputs for Material BNW:

- Concrete mass density = 0.00022 slugs
- Initial tangent modulus = 4,200,000 psi
- Poisson's ratio = 0.18
- Concrete compression strength = 5000 psi
- Concrete cracking capacity = 500 psi (static direct tensile strength)
- Crack width = 2.0000e-04 (at which crack-normal tensile stress goes to zero)
- Aggregate radius = 0.125 inches

Material KCIH will be examined first. Figure E-1-17 shows the displacement load curve used.

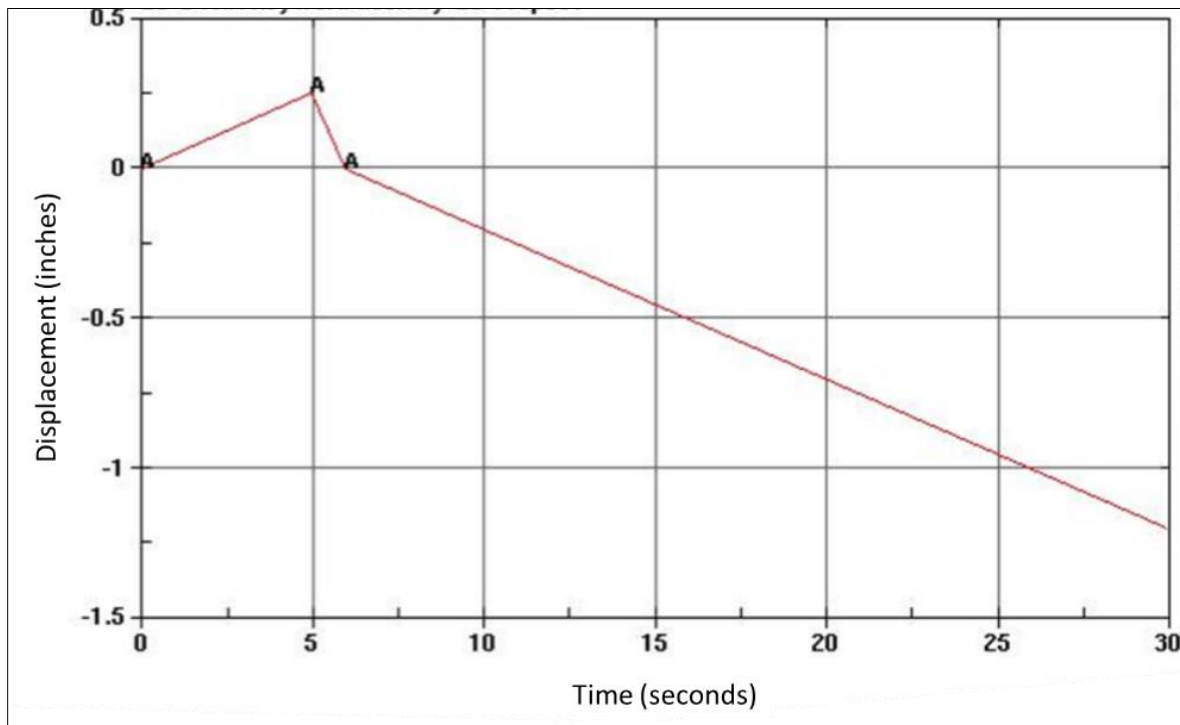


**Figure E-1-17 – Displacement Load Curve**

The column was put into tension over the first 5.0 seconds by extending its length by 0.25 inches. Then it was brought back to its initial length over the next 1.0 second, after which a compressive deformation was applied. Figure E-1-18 shows the stress time history experienced in the column using material KCIH (various locations of stress measurement are chosen and the average is shown).

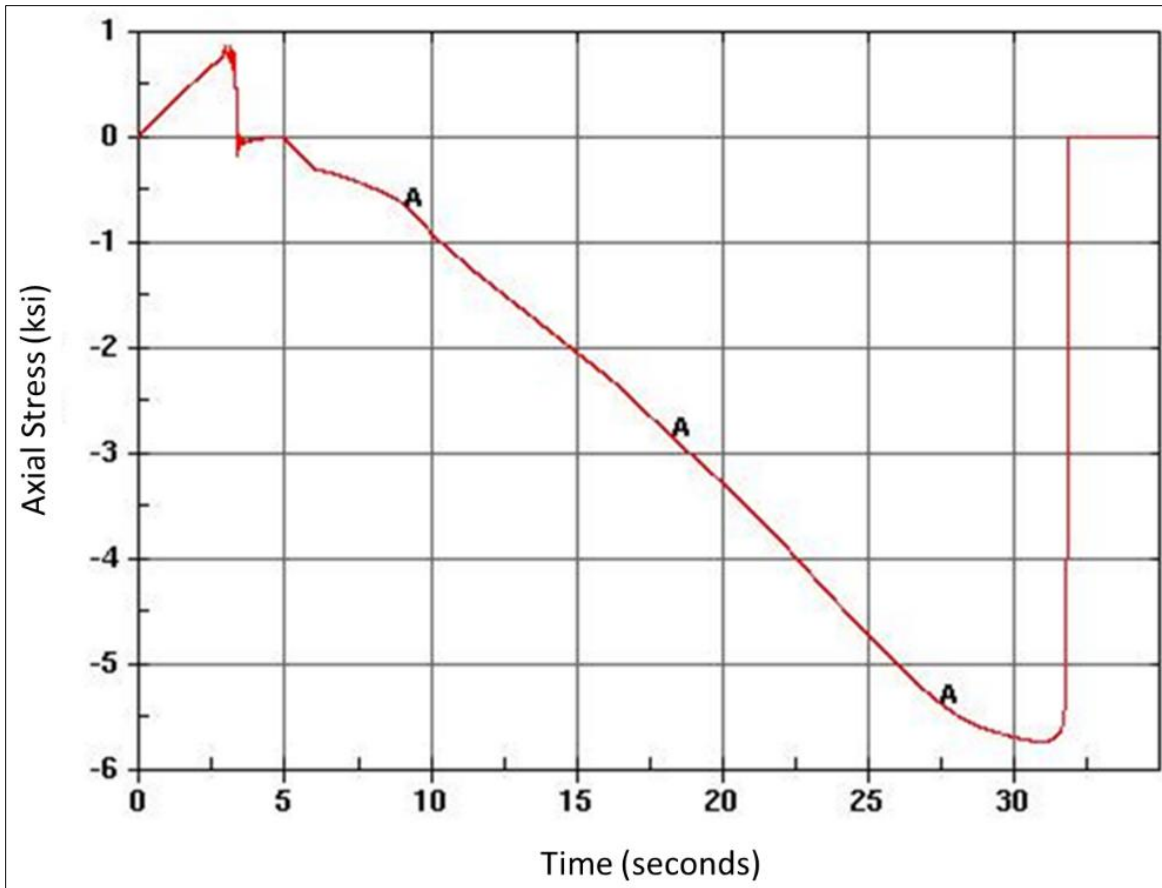


**Figure E-1-18 – Concrete Stress**

As can be seen, as soon as the tensile capacity of the material KCIH is exceeded (at approximately 2.5 seconds), the material fails and becomes stress free. The displacement continues to be applied following the load curve. Since the material failed only in tension previously, it still has compressive capacity. Compressive stresses pick up between 5.0 seconds and approximately 32.0 seconds at which time a compressive failure is experienced. The maximum tensile and compressive stresses appear to be greater than the 500 psi tensile and 5,000 psi compressive limits given. However, this has to do with the influence of the effective strain rate versus shear strength curve given. The faster the load is applied, the higher its effective strength becomes. It was difficult to quantify exactly the rate used to apply the load, however, it should be noted that the recommended effective strain rate versus shear strength curve was used. Figure E-1-19 and Figure E-1-20 show the damage sustained to material KCIH as the column fails in tension and in compression respectively (some of the elastic material is removed to show a cut-away section for visualization).

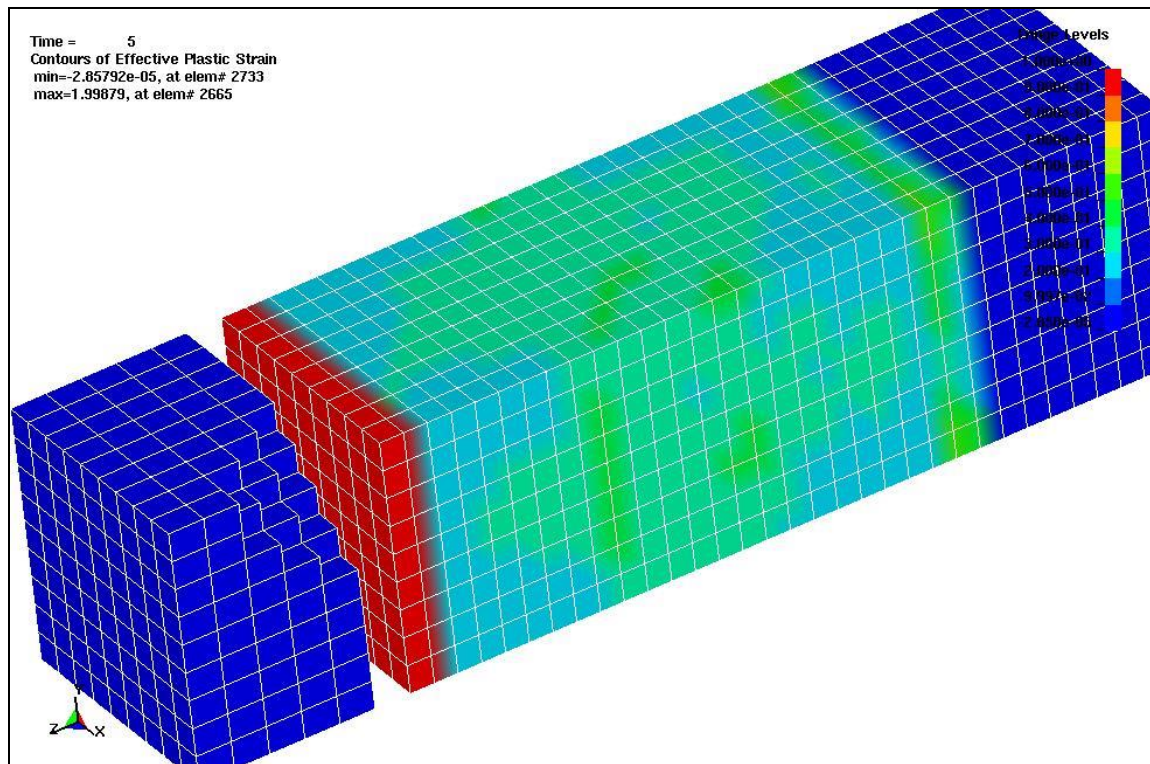


**Figure E-1-19 – Damage at 5.0 seconds**

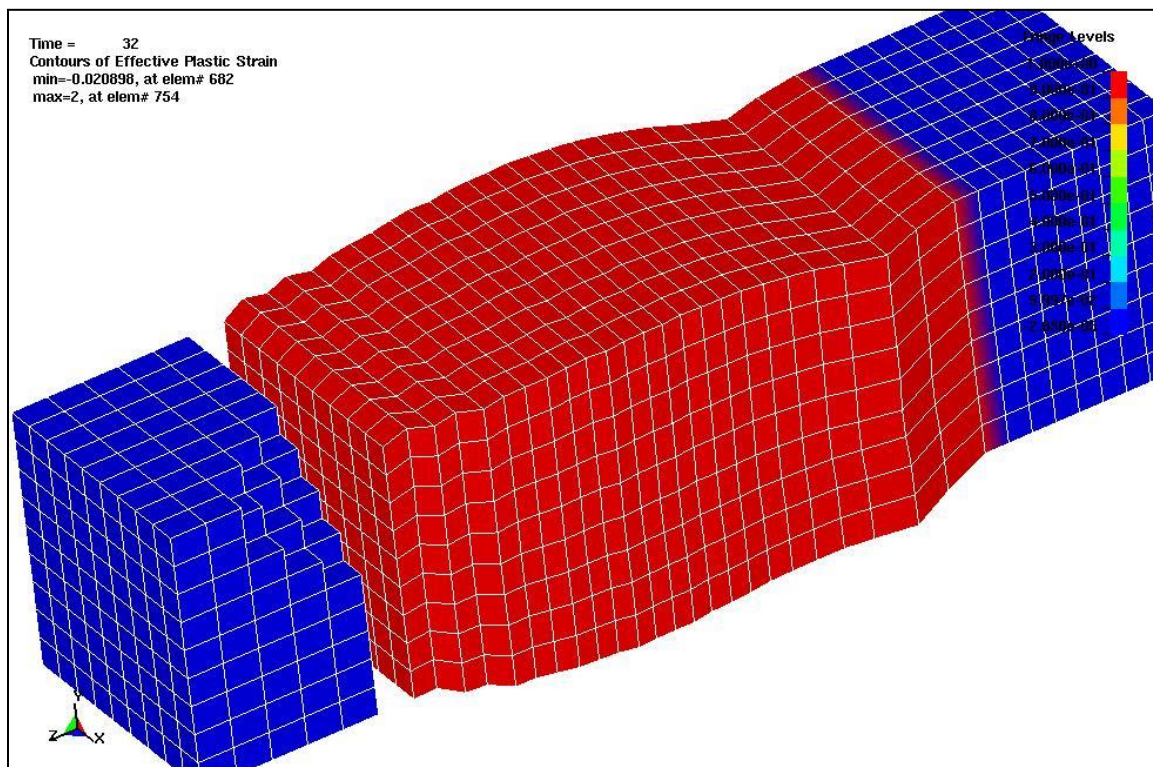


**Figure E-1-20 – Damage at 32.0 seconds**

The damage is displayed on a scale from zero to two (“zero” [blue] indicates no damage, and “two” [red] indicates the element completely cracked or crushed.) At tension failure (Figure E-1-19), only one layer of elements has failed, while at the compression failure (Figure E-1-20), all elements have failed. This compressive failure occurs suddenly. As can be seen, this material behaves as expected. One observation on the damage parameter is that this parameter is cumulative and does not differentiate between compressive or tensile failure. In other words, say the particular element fails in tension first. The damage parameter will be reported as “two”. However, this element has capacity to take compression and can be loaded to a reduced compression limit before sustaining further damage. In the meantime, the damage parameter will continue to be reported as “two” throughout the entire compression loading.

Next, the same load curve is applied to an identical column model using material BNW. The load curve is shown in Figure E-1-17, while the stress time history at various locations is shown in Figure E-1-21.

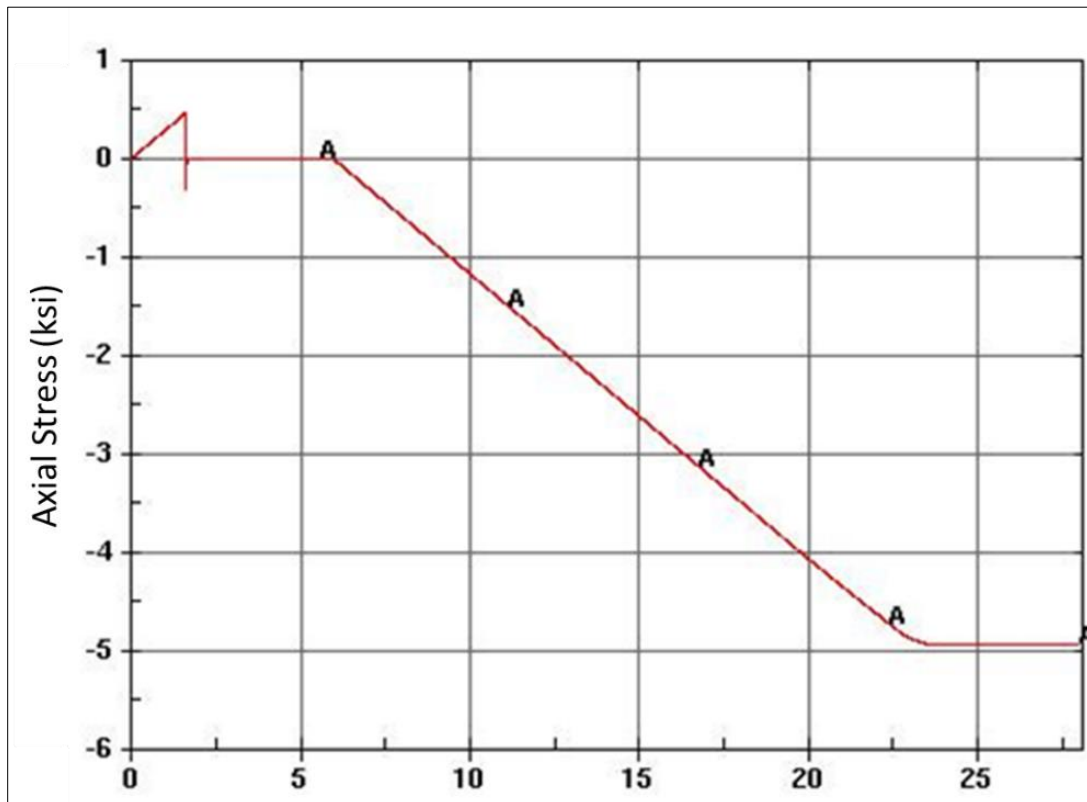


**Figure E-1-21 – Concrete Stress**



The response is similar to material KCIII, however, with material 83, the compressive capacity of the section is not reduced after the compressive limit is attained, just held constant. This is not how concrete behaves in reality where loss of strength is typical after the compressive limit is achieved. However, this is not a big concern, since in most failures of interest, a compression failure is not the controlling failure mode. Figure E-1-22 and Figure E-1-23 show the damage sustained to material BNW as the column fails in tension and in compression respectively. One feature of this material is the graphical depiction of the crack orientations.

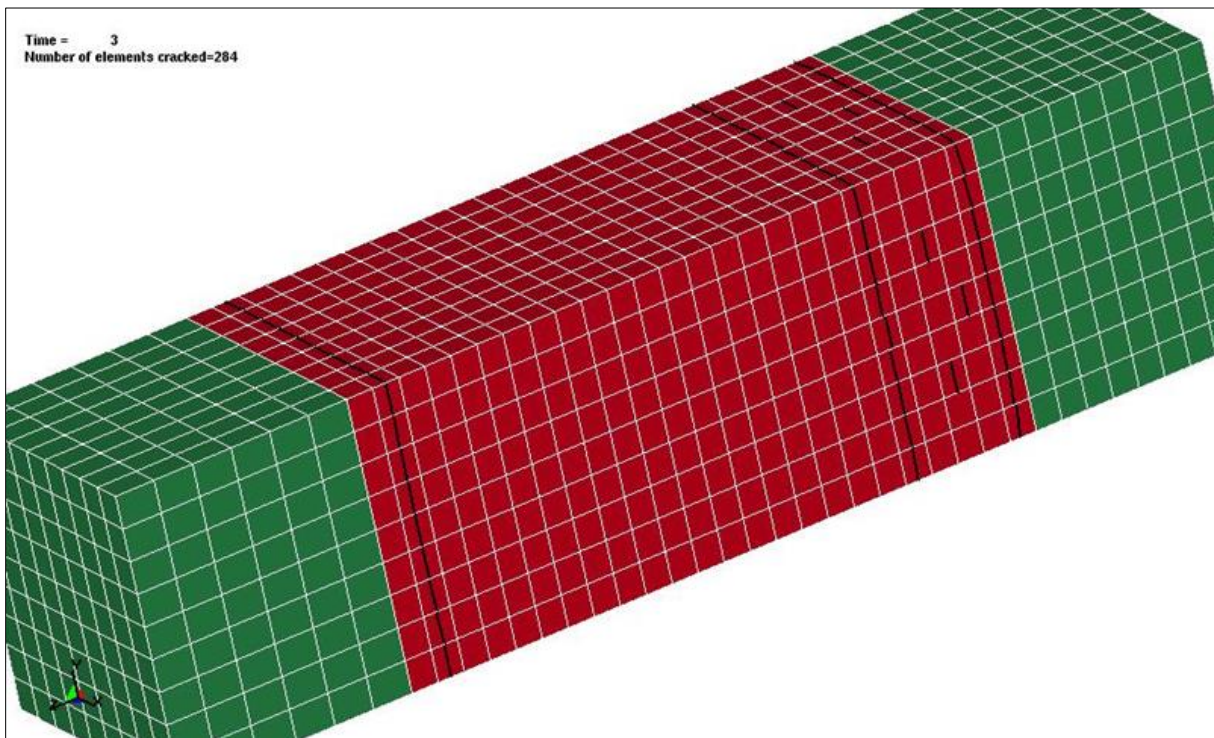


**Figure E-1-22 – Damage at 3.0 Seconds**

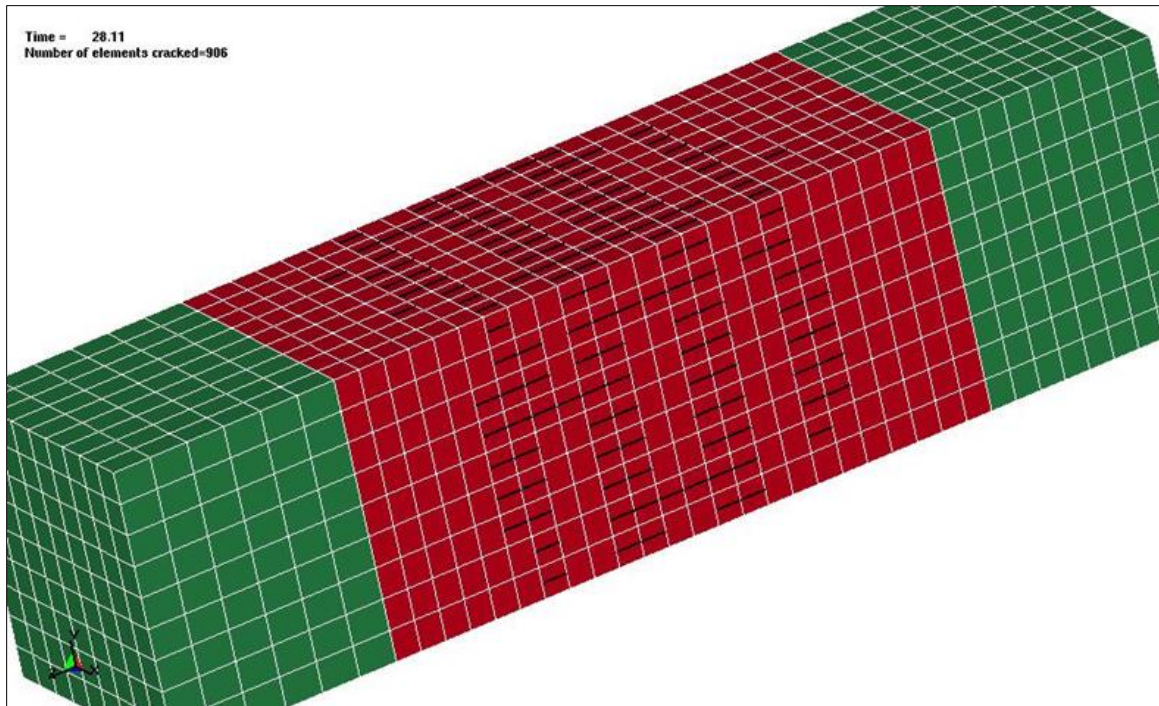


**Figure E-1-23 – Damage at 28.11 Seconds**

Note, in Figure E-1-22, the tension cracks are perpendicular to the section, while in Figure E-1-23, the tension cracks are parallel to the section. This material also behaves as expected, however, with the particular trait that the compressive capacity of the section is not reduced after the compressive limit is attained.

#### **E-1.7.2 Flexure Failure (Beam is Under-reinforced)**

For the flexural validation analyses, the same two material models and critical values were assumed. Also, the tension failure stress was set to a low value (50 psi) as is assumed in classical solutions. In addition, a non-linear material model was used for the reinforcement.

For nonlinear reinforcement model, the material properties are input as follows. The stress/strain curve is shown in Figure E-1-24

- Steel mass density = 0.00073 slugs
- Young's modulus = 29,000,000 psi
- Poisson's ratio = 0.3
- Yield stress = 30,000 psi
- Tangent modulus = 25,000 psi

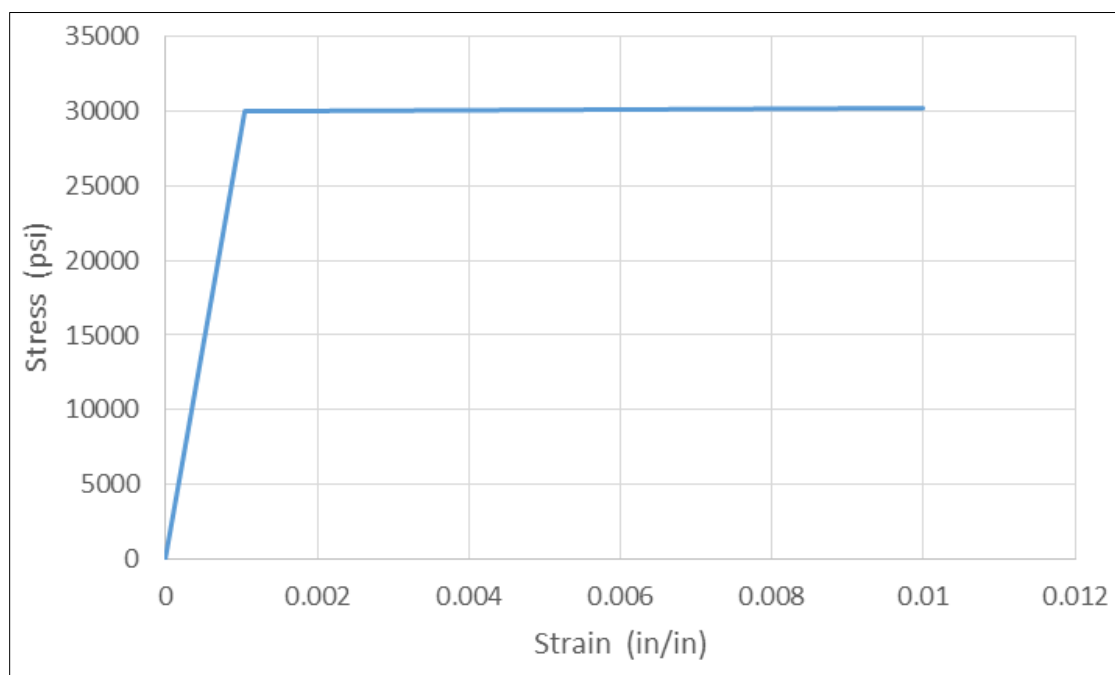


**Figure E-1-24 – Reinforcement Stress Strain Curve**

To demonstrate this failure mode, the beam was loaded with a 120 psi uniform load on the top surface. The reinforcement was sized as 10-inch square bars and failure was computed using concrete design principals at approximately 800 kip-ft/ft, which translates to a uniform load of approximately 61 psi on the top surface. As the uniform load of 120 psi is ramped on from zero to one second, the yield stress of the steel should occur at approximately  $61/120 = 0.5$  seconds.

Material KCIII was tested first. Figure E-1-25 depicts the time history of the rebar force and shows that the rebar yields at approximately 0.5 seconds. Figure E-1-26 shows the time history of the beam displacement at the midpoint.

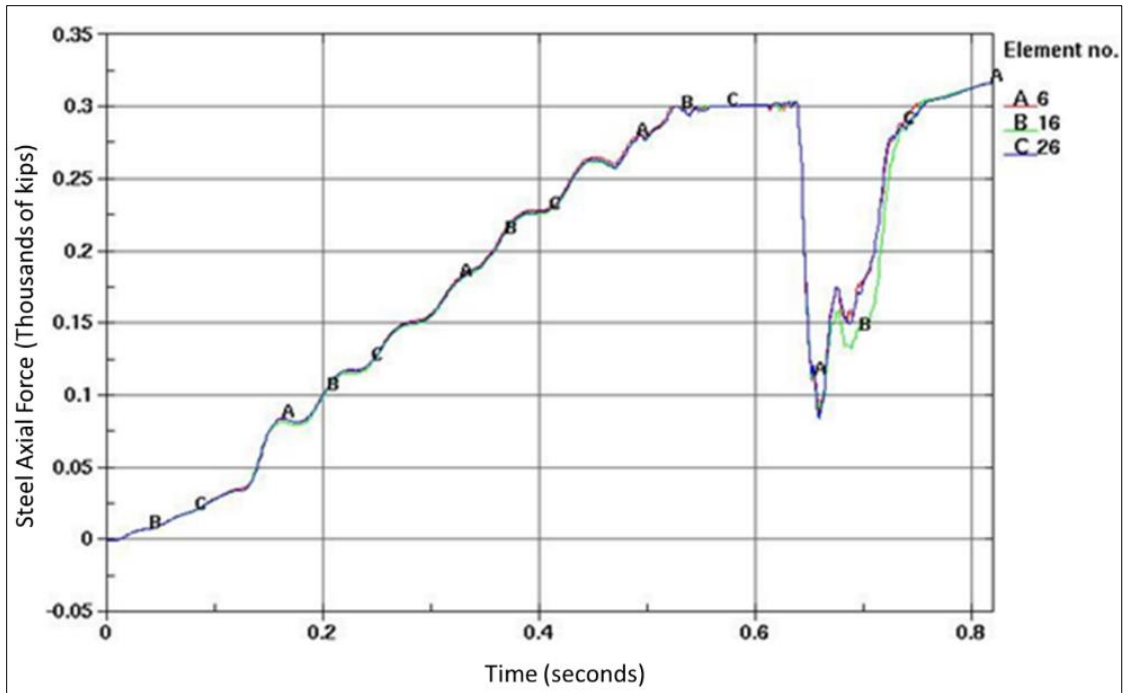


**Figure E-1-25 – Rebar Force Time History**

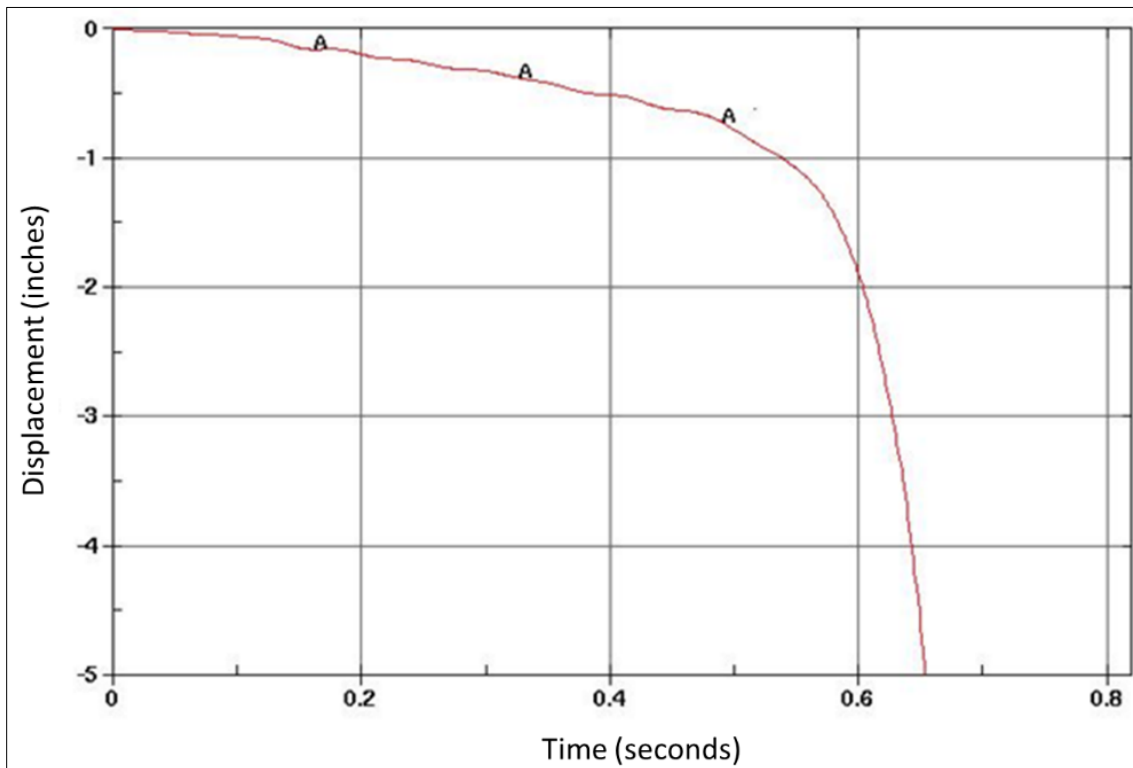


**Figure E-1-26 – Beam Displacement at Midpoint**



As can be seen, the beam deflects approximately 0.75 inches at yield. Figure E-1-27 shows the concrete damage at time of steel yield. The red areas depict the cracking pattern. Figure E-1-28 shows the concrete damage at complete failure. It can be seen that the entire beam is highly damaged, although the output does not differentiate which area is crushing and which area is cracking.

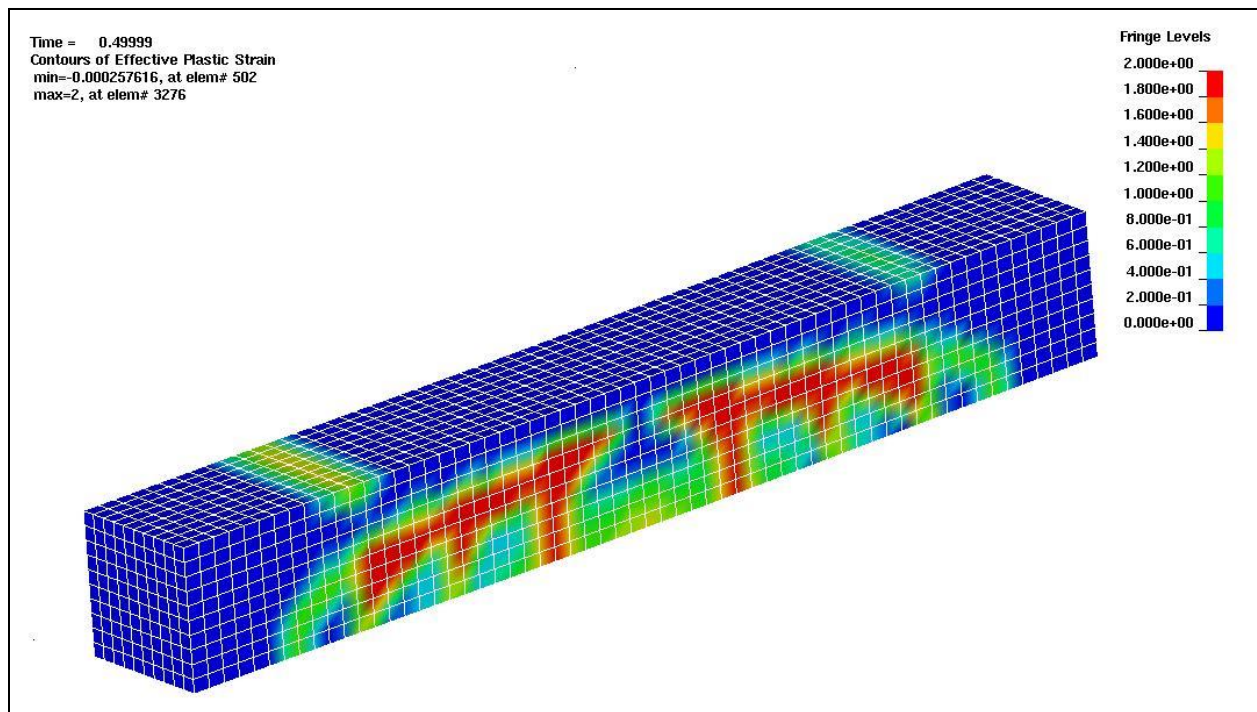


**Figure E-1-27 – Concrete Damage at Rebar Yield**

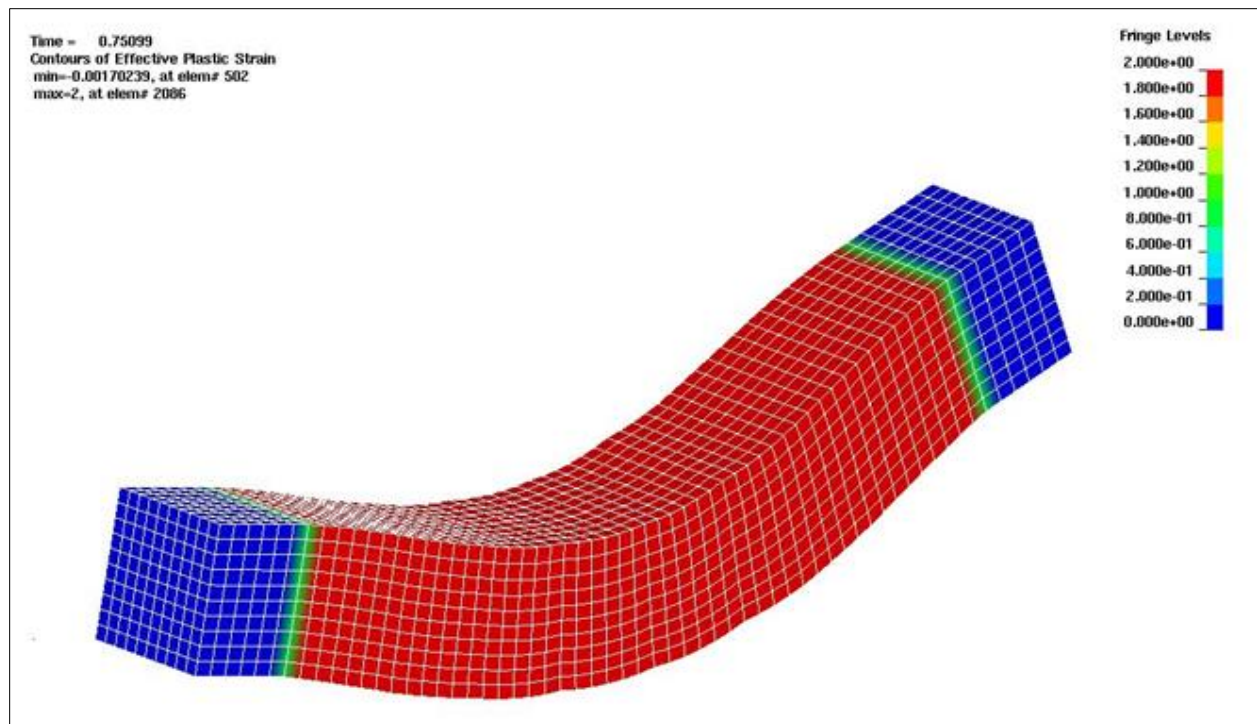


**Figure E-1-28 – Concrete Damage at Complete Failure**

Next, material BNW was tested. Figure E-1-29 depicts the time history of the rebar force and shows that the rebar yields at approximately 0.5 seconds, comparable to the run using material KCIII and in agreement with the classical solution. Figure E-1-30 shows the time history of the beam displacement at the midpoint.

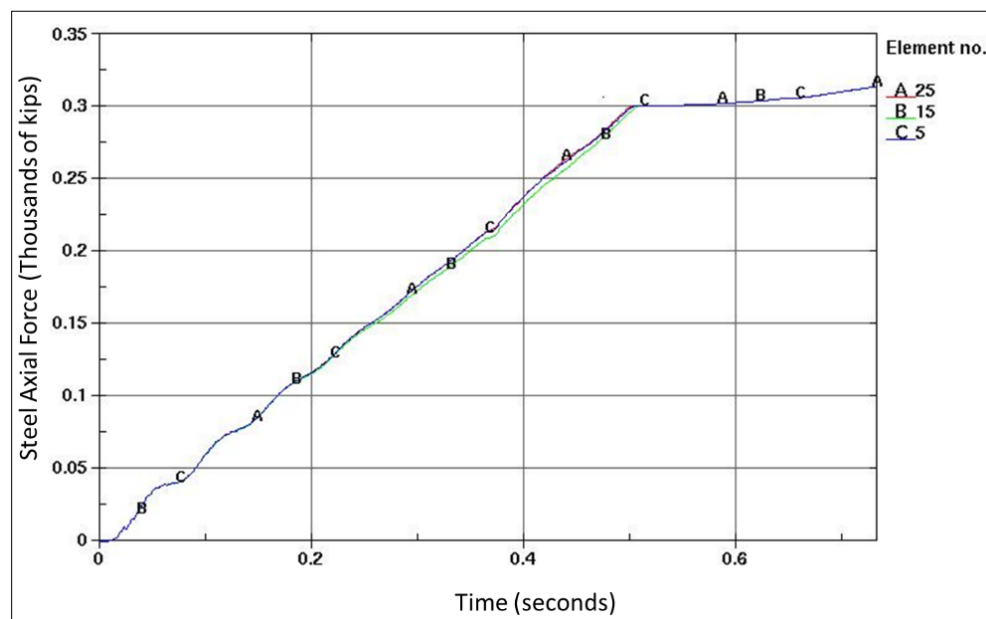


**Figure E-1-29 – Rebar Force Time History**

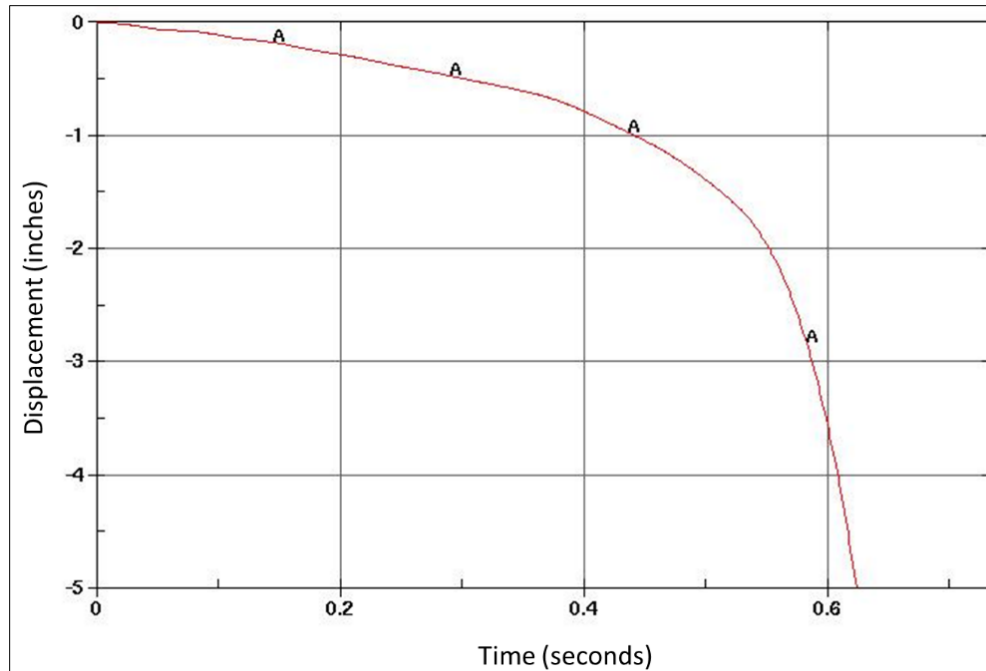


**Figure E-1-30 – Beam Displacement at Midpoint**

As can be seen, the beam deflects approximately 1.5 inches at yield, which is twice that calculated using material KCIII. It should be noted that the aggregate size influences the deflection; a larger aggregate will reduce the deflection. Figure E-1-30 shows the concrete damage at time of steel yield, while Figure E-1-31 shows the concrete damage at complete failure.

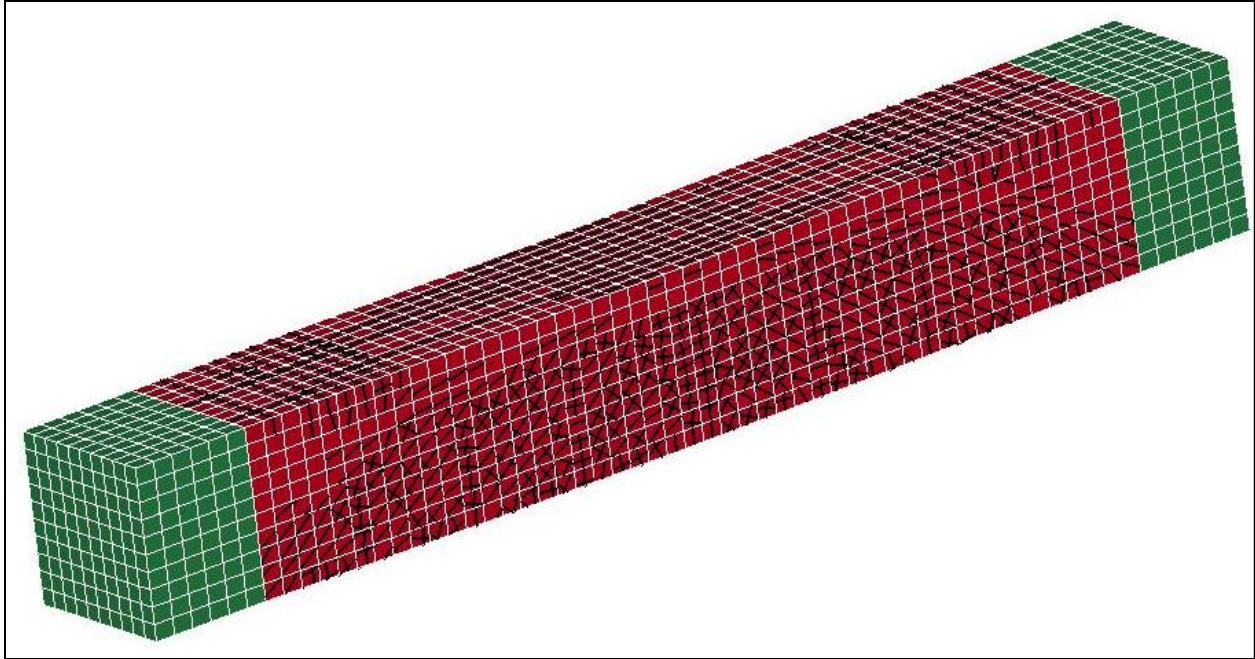


**Figure E-1-30 – Concrete Damage at Rebar Yield (0.5 seconds)**

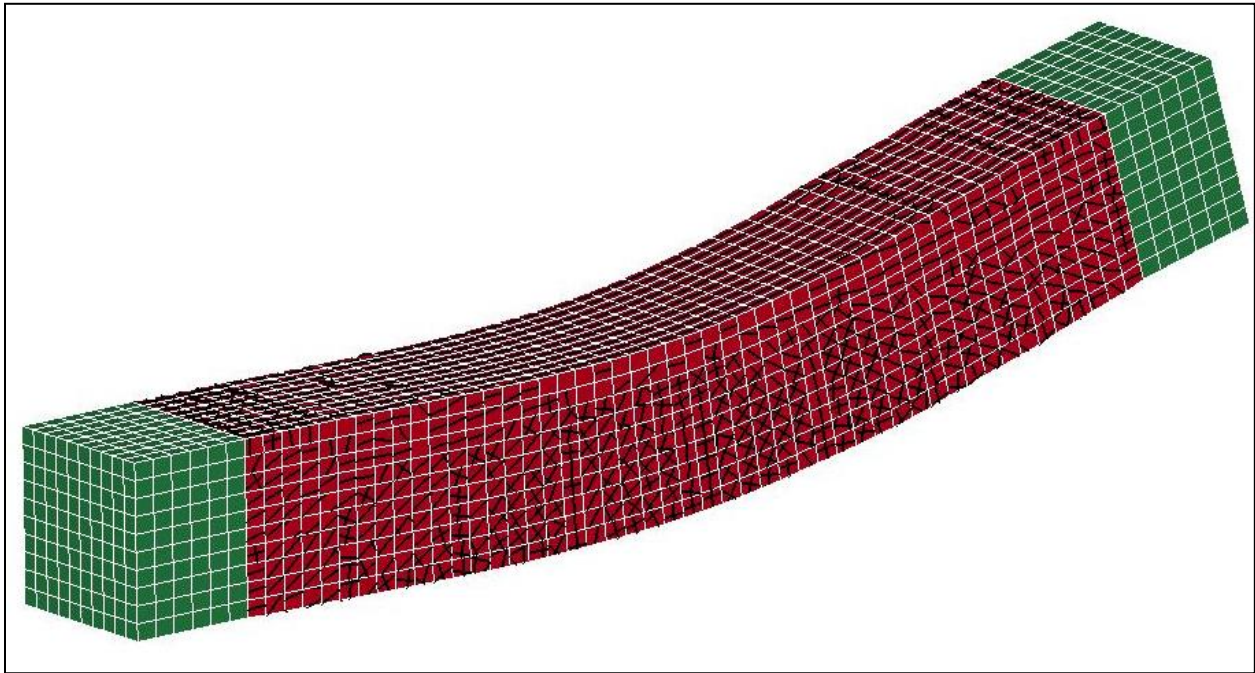


**Figure E-1-31 – Concrete Damage at Complete Failure (0.733 seconds)**

### **E-1.7.3 Concrete Crushing Failure (Beam is at Balanced Condition)**

To demonstrate this failure mode, the beam reinforcement was increased in order to achieve a balanced condition and the beam load was increased in order to force the concrete to crush.

Based on the following equation from reinforced concrete design principles:

$$A_s f_y = 0.85 f'_c A_c$$

Where  $A_s$  = steel area of reinforcement  
 $f_y$  = yield strength of steel  
 $f'_c$  = compressive strength of concrete  
 $A_c$  = area of fully developed concrete compression block

With the given cross section of this test beam, about 49 in<sup>2</sup> of reinforcement is required to achieve the balanced condition, sustaining a load of 390 psi loading.

First, material BNW was used. With approximately 42 in<sup>2</sup> of steel, the reinforcement started to yield at the same time the concrete started to crush, thus achieving a balanced condition. This occurred at time 0.33 seconds of ramping on a 1,000 psi uniform pressure (330 psi load). Any amount of rebar less than 42 in<sup>2</sup> resulted in the steel yielding too soon; a more ductile behavior.

Figure E-1-32 shows the concrete cracking pattern at this balanced condition (the beam is cut at midspan with only half of the beam shown). A finer mesh was required in order to capture this behavior (elements on the order of 2 inch in size). Figure E-1-33 shows this same concrete cracking pattern but with principal stress vectors superimposed. Theoretically, the compression block should have a nonlinear stress distribution from top to bottom. However, as shown previously, with material BNW, compressive capacity at any particular point is not reduced after the compressive limit is attained, just held constant. This is observed in Figure E-1-33. The compression block is a little more than 1/3 of the beam depth and the compression stresses are fairly uniform over the height. Material model KCIII would be expected to give a more non-linear stress distribution as would be expected in reality.



Time = 0.33199  
Number of elements cracked=19010

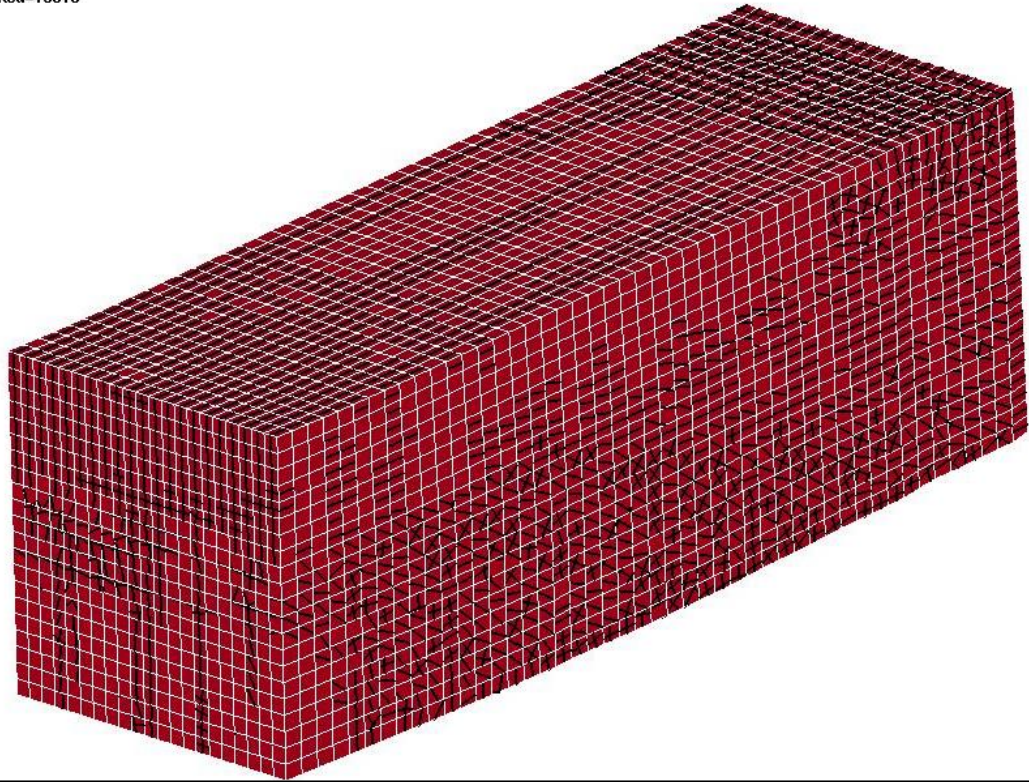


**Figure E-1-32 – Concrete Cracking Pattern at Failure**

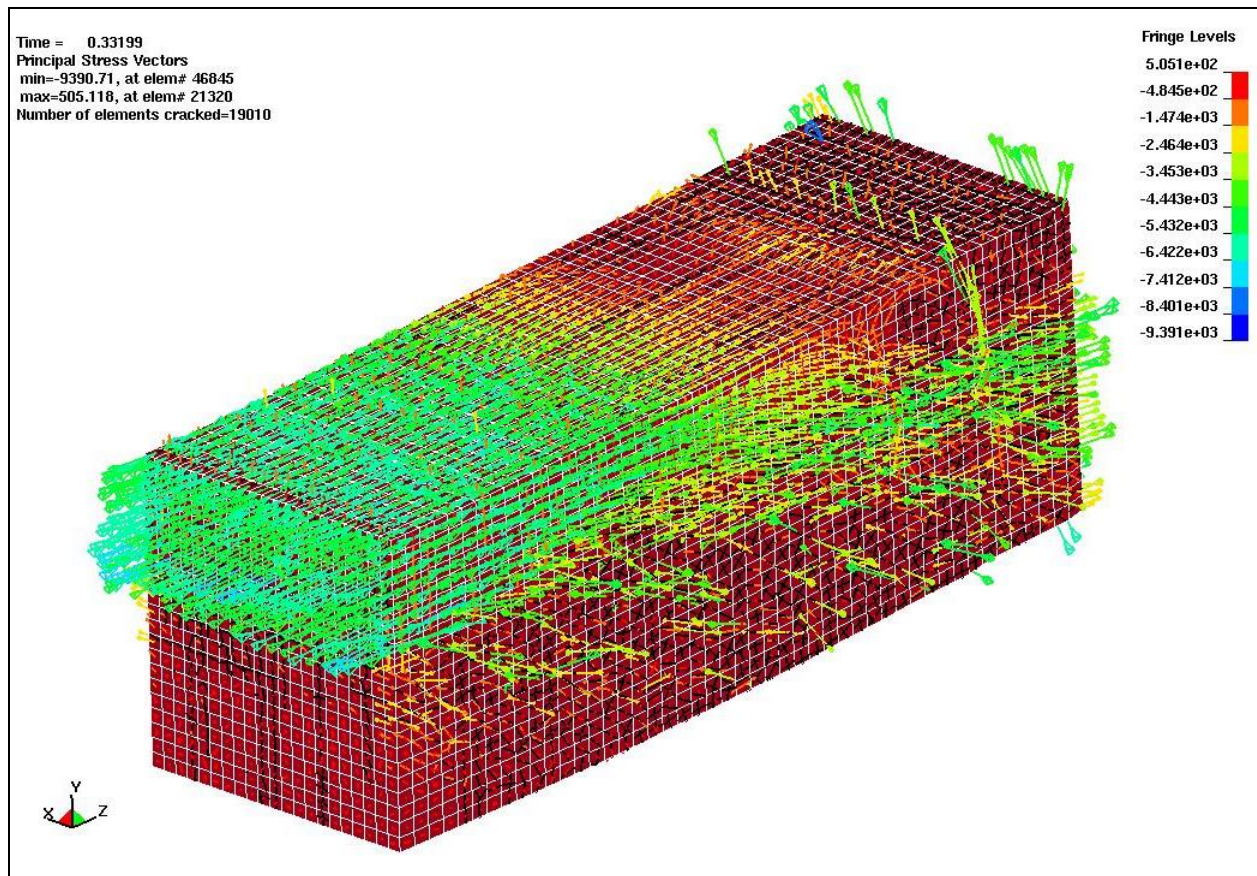


**Figure E-1-33 – Concrete Cracking Pattern + Principal Stress Vectors at Failure**

Figure E-1-34 shows the force in the reinforcement. As can be seen, the reinforcement starts to yield at approximately 0.33 seconds. Reasonable tension values are required to be used in the concrete material model. For this run, 1/10 of the compressive stress was input. If low values are used, crushing is not achieved because the beam cannot maintain its integrity.

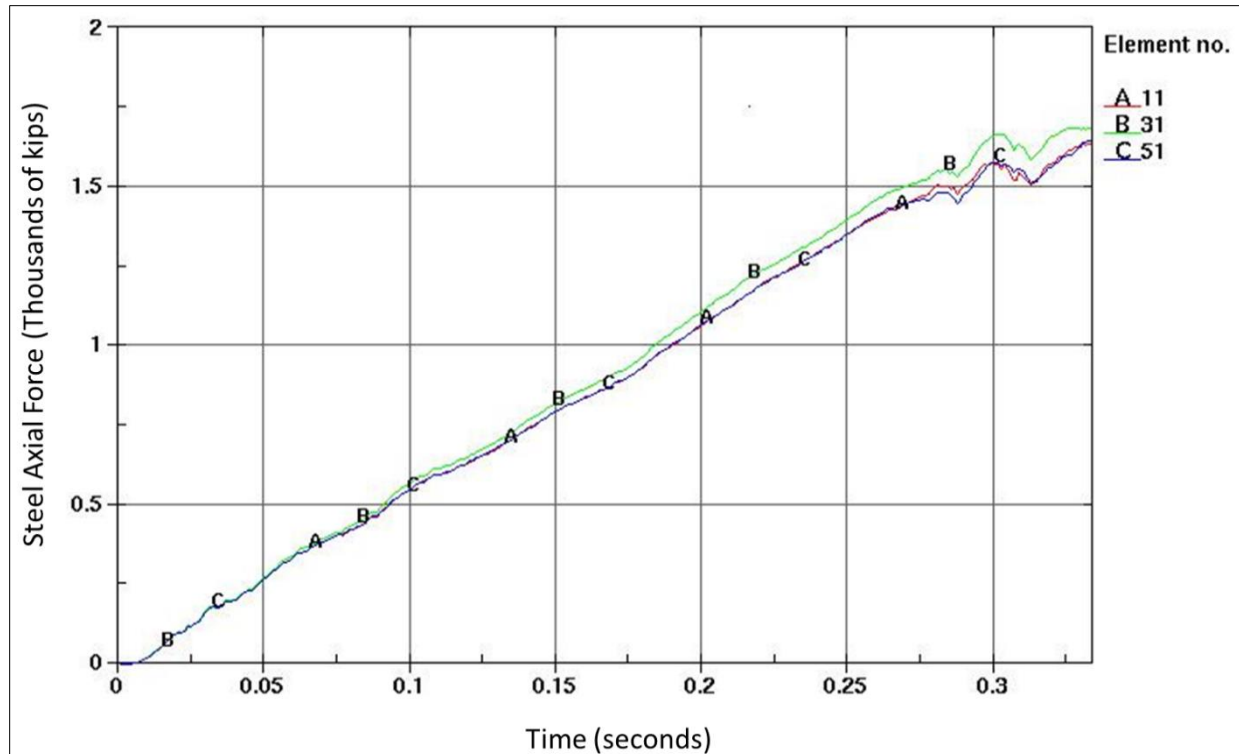


**Figure E-1-34 – Rebar Force Time History**

Next, material KCIII was used. This time the 1,000 psi load was ramped on over 10 seconds. Beam crushing was achieved at approximately 1.7 sec (170 psi load). Figure E-1-35 shows the concrete damage right before crushing.



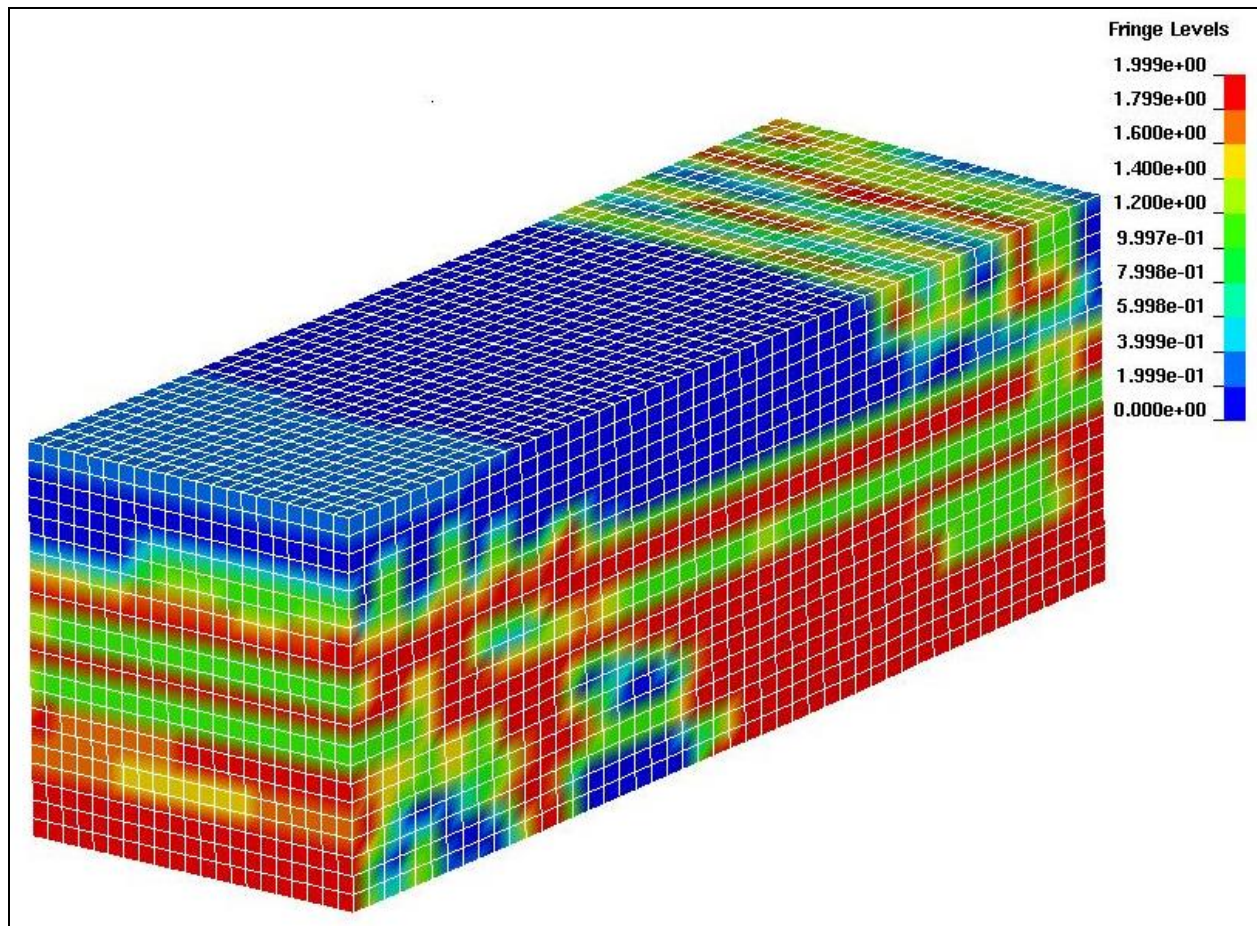


**Figure E-1-35 – Concrete Damage at Time of Crushing (1.66 seconds)**

It is peculiar that the crushing occurred so early compared with the beam using material BNW. Upon further investigation, it appears that once material KCIII reaches the compressive limit, all residual strength is significantly reduced. Not so with material BNW. This difference in the behavior between the materials is shown in Figure E-1-36 and Figure E-1-37 and is similar to that found when testing the concrete column described previously in this section. The elements plotted start at the top of the section (element 27331) and end at the 6<sup>th</sup> element at depth (element 27226) in order to represent most of the compression block.

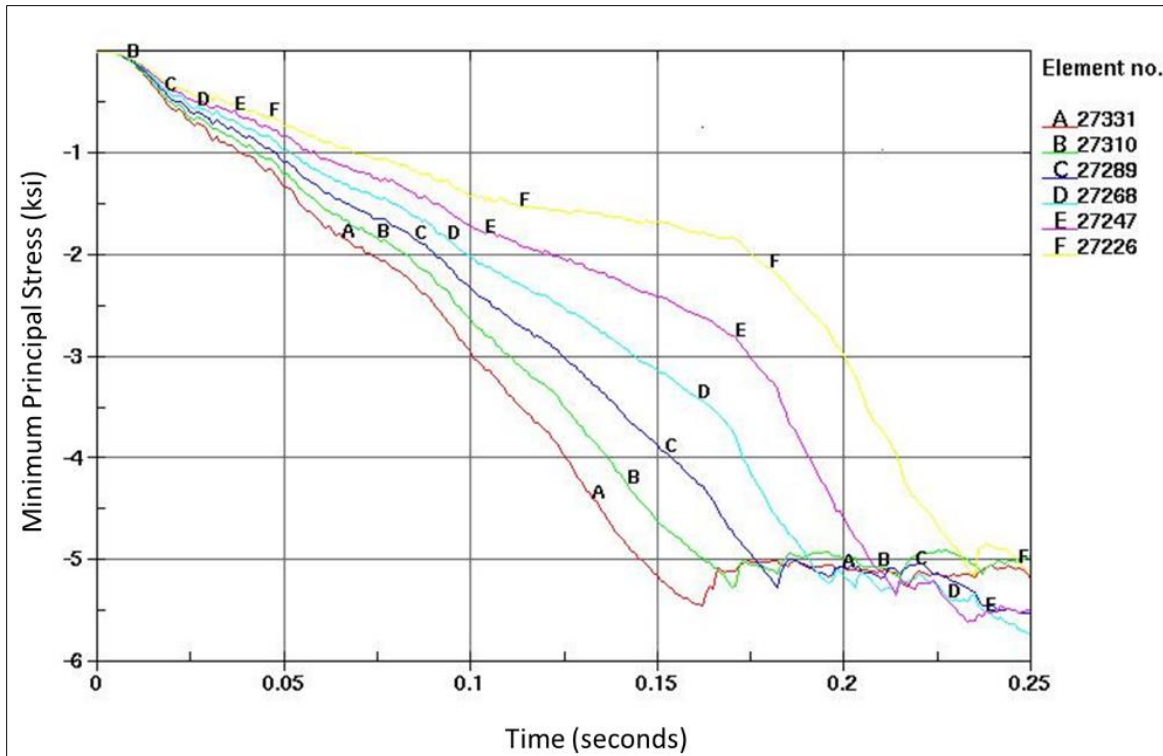


**Figure E-1-36 – Minimum Principal Stresses (Mat BNW)**

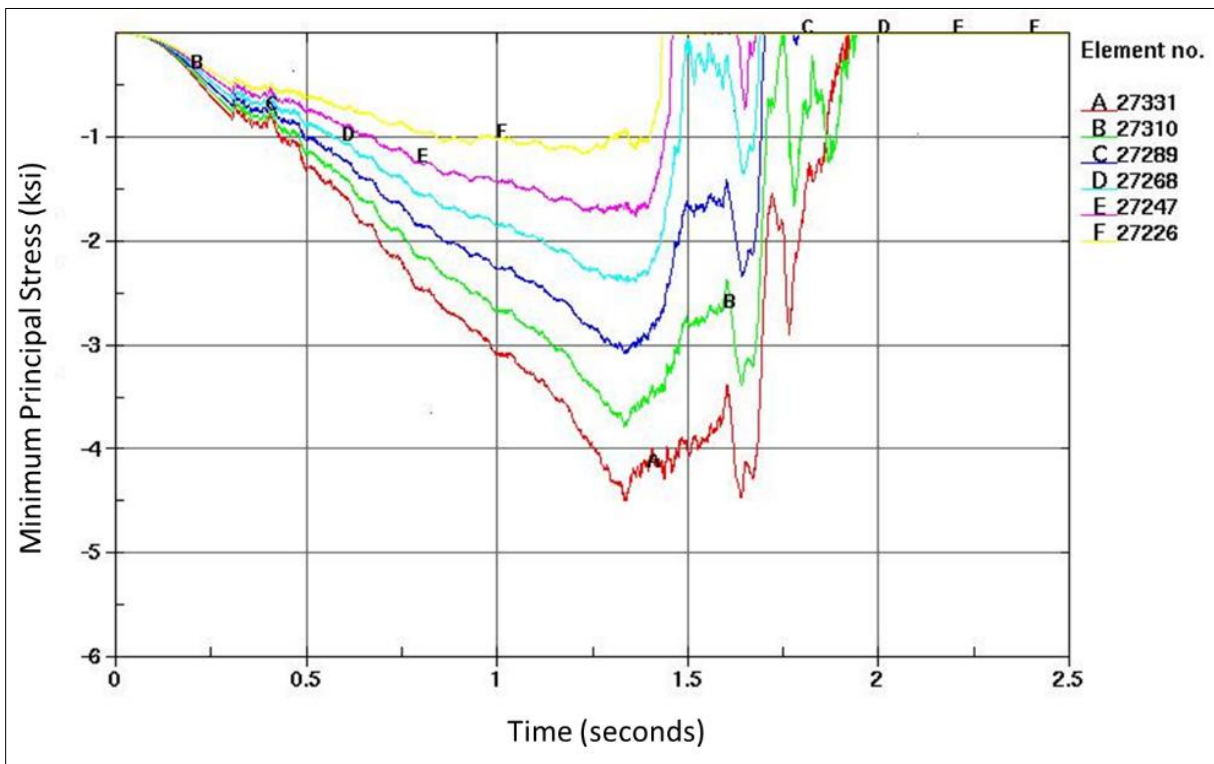


**Figure E-1-37 – Minimum Principal Stresses (Mat KCIII)**

Both runs have elements that reach compression failure at approximately 150psi of the applied load. Elements that use material KCIII quickly lose the capacity shortly after reaching the compressive limit. The elements using material BNW maintain stress until eventual failure at approximately 33% of the applied load. Again, this difference between material behaviors may not be important, since most of the failures of interest involve mass concrete or under-reinforced sections and crushing is typically not an issue.

#### **E-1.7.4        Shear Failure**

Beam shear is an engineering term used to signify that a shear force is a more significant contributor at the particular location of a structure than in a location where the behavior is governed more by bending. This results in the principal stresses at that location being oriented at an inclined angle. For unreinforced concrete, the failure of the beam will occur when the principal stresses exceed the tensile capacity of the concrete. If the beam only has longitudinal steel, the reinforcing will control the cracking to some degree and allow for friction within the cracks in addition to the strength of the intact concrete in the compression block. The longitudinal steel will also add some resistance due to dowel action across the cracks. Stirrups in the concrete further increase the strength by controlling the diagonal cracking and by absorbing the inclined principal stresses as longitudinal stress in the upright portions of the stirrups. The above sections exercised the performance of the concrete material models in compression, tension and bending, thus subjecting the models to a variety of different principal stress orientations. These sections demonstrated that the tensile strength and crack development are highly dependent on the assumptions made in the particular material model.

This may not be an issue in many cases where the structures being evaluated are massive structures placed in lifts. The lift joints create weak planes in the concrete which must be modelled explicitly to capture the shear strength of the structure. The potential shear planes can be modelled using contacts. Tie-break contacts can be used to model bonded lift joints. The contact will effectively tie the two faces of concrete together until the input tensile and/or shear strength is reached, at which point the material will crack along the contact geometry. Once the contact is cracked through, sliding will be allowed utilizing the input sliding friction value.

Sliding contacts can be used to model unbonded lift joints or contraction joints. These contacts behave essentially the same as tie-break contacts with zero tensile strength.

#### **E-1.7.5 Concrete Test Results Summary**

Both concrete material models were evaluated for a variety of conditions ranging from axial tension and compression to flexural bending with different percentages of reinforcement steel. Input parameters for these models is obtained as discussed in the previous sections. In general, if the reinforcement controlled (failure governed by reinforcement yielding), the tests showed close agreement with theoretical solutions. However, if concrete tension or compression is the main failure mode, results are highly dependent on the assumptions made in the particular material model formulation. Since concrete structures are generally designed as under reinforced or as mass concrete, these concrete dominated failure modes do not control and the use of these material models is acceptable. In cases where tension and shear control, such as at lift joints, contacts can be used in conjunction with linear or non-linear material models to accurately model the behavior of the structure.

#### **E-1.8 Using Concrete Properties for Risk Analyses**

When conducting a risk analysis it is necessary to estimate the probability of failure of concrete structures. One convenient method for doing this is to perform a Monte Carlo analysis. This will require determining probability distributions for each parameter. If there is enough test data, this can inform the development of distributions. In cases where test data is lacking the compressive strength can be used to estimate most other parameters. Based on field data on the compression strength, site specific cores, or standard values defining the variability of concrete, a distribution on the compression strength can be determined. From this, distributions for the correlated parameters follow directly. For shear strength parameters, the data from Figure E-1-14 can be used to set reasonable distributions for the friction angle and cohesion intercept within the normal stress range of interest. Once distributions have been set, they can generally be used in a static analysis or in simplified dynamic analyses. For more complex dynamic analysis, the computation time is generally too extensive to incorporate a full Monte-Carlo analysis. For this reason, dynamic analyses are generally run for mean values with some limited sensitivity to define the range of response, from which a probability of failure can be estimated.

### E-1.9 Example Problem

A concrete gravity dam was built 62 years ago. The complete construction records have been lost over the years and it is unknown if the specified compressive strength of the concrete was. Construction photos are available which seem to indicate good lift joint cleanup and concrete placement practices. The specifications are not available but the notes on one of the drawings indicate that type II cement was used. Near the end of construction instrumentation was installed in the dam which required that the concrete was cored at numerous locations along the length of the dam. These cores were tested at the time for compressive strength and showed an average strength of 2700 psi. Many of these cores crossed several lift joints. From the photos available of the cores, approximately 90% of these showed a bonded lift joint. It is estimated that the cores were drilled approximately 1 year after the concrete was placed. Since the design, the seismic loading in the area has increased. An initial linear elastic finite element analysis is to be run to determine the risk of failure during an earthquake. Estimate the modulus of elasticity and the tensile strength of the mass concrete to be used in this dynamic linear elastic finite element analysis.

#### Possible Solution

First, estimate the current day compressive strength. The cement type is stated to be type II, therefore the coefficient in Equation E-1-1 is 0.477. The current compressive strength is then:

$$f_{c,62} = 2700e^{0.477\left(1-\sqrt{\frac{1}{62}}\right)} = 4095 \text{ psi}$$

From this the modulus of elasticity can be estimated using Equation E-1-2. Since the unit weight is not given, assume it is halfway between 150 and 155 pcf, or 152.5 pcf. This represents the instantaneous modulus and can therefore be used for the dynamic analysis.

$$E = 33(152.5^{1.5})\sqrt{4095} = \mathbf{3.98 \times 10^6 \text{ psi}}$$

The splitting tensile strength can be estimated from Equation E-1-5.

$$\sigma_t = 1.7(4095)^{2/3} = 435.1 \text{ psi}$$

This represents the static splitting tensile strength of parent concrete for a mix with small aggregate. The dynamic modulus of rupture is needed for mass concrete at a lift joint. Though aggregate size was not stated in the problem, assume it has large aggregate since it is mass concrete. Given the performance of the lift joints from the coring, assume that the lift joints were well prepared. Based on Table E-1-3, the following correct factors are used:

Splitting Tension to Direct Tension = 0.8

Direct Tension to Apparent Linear Strength (Modulus of Rupture) = 1.33

Well Prepared Lift Joint = 0.85

Large Aggregate = 0.9

Rapid Loading = 1.5

This results in a total multiplier of  $0.8(1.33)(0.85)(0.9)(1.5) = 1.22$

The tensile strength to use in interpreting the linear elastic analysis is  $435.1(1.22) = \mathbf{531 \text{ psi}}$

## E-1.10 References

- ACI 211. (1991 (reapproved 2009)). *Standard Practice for Selecting Proportions for Normal, Heavyweight, and Mass Concrete*. Farmington Hills, MI: American Concrete Institute (ACI).
- ACI 214. (2011). *Guide to Evaluation of Strength Test Results of Concrete*. Farmington Hills, MI: American Concrete Institute (ACI).
- ACI 318. (2014). *Building Code Requirements for Structural Concrete*. Farmington Hills, MI: American Concrete Institute (ACI).
- ASTM. (2014). *Standard Test Method for Static Modulus of Elasticity and Poisson's Ratio of Concrete in Compression*. West Conshohocken, PA: ASTM International.
- ASTM. (2016). *Standard Test Method for Flexural Strength of Concrete (Using Simple Beam with Third-Point Loading)*. West Conshohocken, PA: ASTM International.
- ASTM. (2017). *Standard Test Method for Splitting Tensile Strength of Cylindrical Concrete Specimens*. West Conshohocken, PA: ASTM International.
- Cannon, R. W. (1995). *Appendix E, Tensile Strength of Roller Compacted Concrete*. Washington DC: US Army Corps of Engineers.
- Dolen, T. P., Harris, D. W., & Nuss, L. K. (2014). Tensile Strength of Mass Concrete - Implications of Test Procedures and Size Effects on Structural Analysis of Concrete Dams. *Dams and Extreme Events - Reducing Risk of Aging Infrastructure under Extreme Loading Conditions*. San Francisco, CA: US Society on Dams (USSD).
- Ghanaat, Y. (2002). Seismic Performance and Damage Criteria for Concrete Dams. *Third US-Japan Workshop on Advanced Research on Earthquake Engineering for Dams* (pp. 151-165). San Diego, CA: US Army Corps of Engineers.
- Livermore Software Technology Corporation. (2012). LS-DYNA - Version 971. Livermore, CA.
- Malaikah, A., Al-Saif, K., & Al-Zaid, R. (2004). Prediction of the Dynamic Modulus of Elasticity of Concrete under Different Loading Conditions. *International Conference on Concrete Engineering and Technology*.
- Malvar, J. L., & Crawford, J. E. (1998). Dynamic Increase Factors for Concrete. *Twenty-Eight DDESB Seminar*. Orlando, FL: Naval Facilities Engineering Services Center.

- Min, F., Yao, Z., & Jiang, T. (2014). Experimental and Numerical Study on Tensile Strength of Concrete under Different Strain Rates. *The Scientific World Journal*.
- Mohorovic, C., Harris, D., & Dolen, T. (1999). *Dynamic Properties of Mass Concrete Obtained from Dam Cores*. Denver, CO: US Bureau of Reclamation.
- Raphael, J. M. (1984). Tensile Strength of Concrete. *ACT Journal*, 81(2), 158-165.
- Rocco, C., Guinea, G. V., Planas, J., & Elices, M. (1999). Size Effect and Boundary Conditions in the Brazilian Test: Experimental Verification. *Materials and Structures*, 210-217.
- Saucier, K. L. (1977). *Dynamic Properties of Mass Concrete*. Vicksburg, MS: US Army Engineer Waterways Experiment Station.
- Scott, G. (1982). *Dynamic Response of Jointed Rock Masses, Master's Thesis*. Denver, CO: University of Colorado.
- Stone and Webster Engineering Corporation. (1992). *Uplift Pressures, Shear Strengths, and Tensile Strengths for Stability Analysis of Concrete Gravity Dams*. Denver: Electric Power Research Institute.
- Timoshenko, S., & Goodier, J. N. (1951). *Theory of Elasticity, Second Edition*. York, PA: McGraw Hill.
- Tynes, W. O., & McCleese, W. F. (1973). *Investigation of Methods of Preparing Horizontal Construction Joints in Concrete*. Vicksburg, MS: US Army Engineer Waterways Experiment Station.
- USACE. (1995). *Seismic Design Provisions for Roller Compacted Concrete, EP 1110-2-12*. Washington, D.C.: US Army Corps of Engineers (USACE).
- USACE. (2002). *Coastal Engineering Manual, EM 1110-2-1100*. Washington D.C.: US Army Corps of Engineers (USACE).
- USACE. (2003). *Time-History Dynamic Analysis of Concrete Hydraulic Structures, EM 110-2-6051*. Washington, D.C.: US Army Corps of Engineers (USACE).
- USACE. (2007). *Earthquake Design and Evaluation of Concrete Hydraulic Structures, EM 1110-2-6053*. Washington, D.C.: US Army Corps of Engineers (USACE).
- USBR. (1981). *Concrete Manual*. Denver, CO: US Bureau of Reclamation (USBR).



USBR. (2005). *Roller-Compacted Concrete - Design and Construction Considerations for Hydraulic Structures*. Denver, CO: US Bureau of Reclamation (USBR).

USBR. (2013). *State-of-Practice for the Nonlinear Analysis of Concrete Dams*. Denver: USBR.

Zhou, Y., Tian, H., Sui, L., Xing, F., & Han, N. (2015). Strength Deterioration of Concrete in Sulfate Environment: An Experimental Study and Theoretical Modeling. *Advances in Materials Science and Engineering*.